Doctoral Dissertation

# Studies on Brown Adipose Tissue Fabrication by Controlling Cell Microenvironments via Polymer Nanocoating

Aslı Sena Karanfil

July 2024

Graduate School of Engineering
Osaka University

# Content

# General Introduction

Tissue engineering is a crucial discipline within regenerative medicine, integrating the skills of scientists, physicians, and engineers to create or reconstruct human tissue using living cells, particularly stem cells, for the purpose of repairing, replacing, maintaining, or enhancing specific tissues or organs.[1,2] Initially defined in 1993, tissue engineering utilizes biodegradable polymers as scaffolds for cell culture, which are then implanted into the body to replace damaged tissues.[3] Cells are first isolated from the donor, expanded, and then seeded onto or within a biocompatible tissue scaffold. This structure is subsequently developed using biochemical factors and/or mechanical stimuli, often within a bioreactor. The resulting three dimensional (3D) engineered tissue can then be implanted into the damaged area to promote healing.[4]

Recent advancements have introduced new concepts such as scaffold-free architectures and cell-free approaches, which use specialized biomaterials or cell sheets to promote tissue regeneration.[4] The schematic illustration of tissue engineering is demonstrated in **Figure 1**.

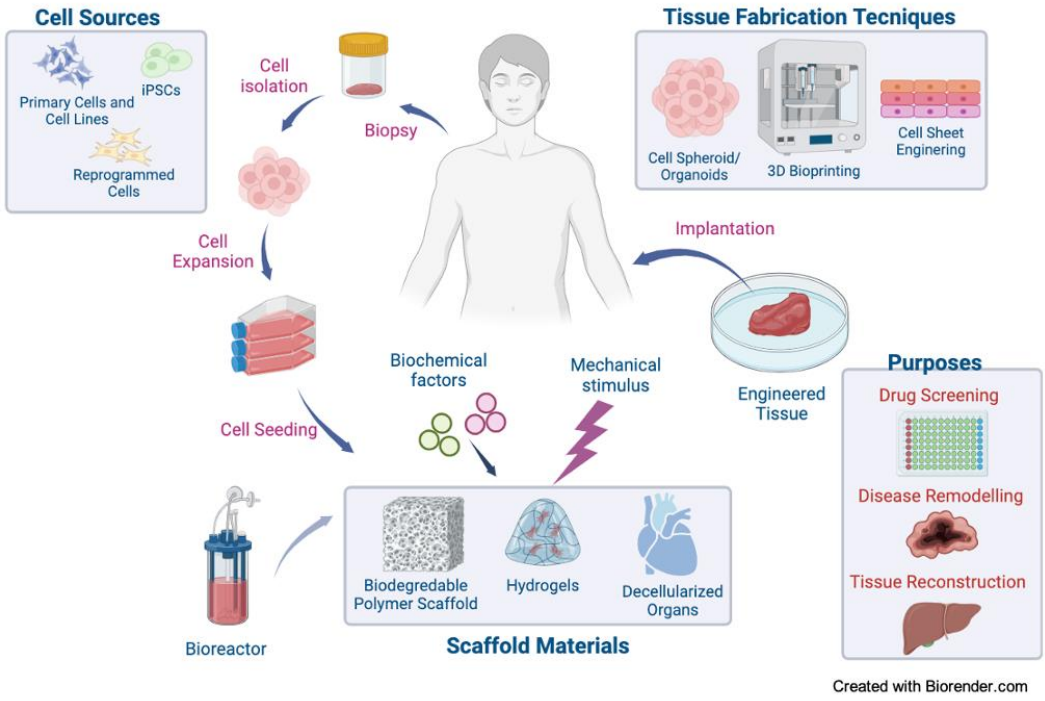


**Figure 1.** Schematic illustration of tissue engineering

Developments in regenerative medicine and tissue engineering have enabled the 3D fabrication of living tissues *in vitro* and diversified approaches to soft tissue engineering.[5–7] This progress is particularly significant given the global rise in obesity and related metabolic comorbidities, which has increased the importance of studying adipose tissue.[8–10] Adipose tissue, comprising 10–30% of total body weight, plays a crucial role in regulating body homeostasis through its endocrine and secretion functions. The main cells in adipose tissue, called adipocytes, act as energy stores due to the high lipid content in their cytoplasm.[11]

There are essentially two main types of adipose tissue: white and brown.[12,13] However, various other types and characteristics of adipose tissue, such as beige, bright, pink, and yellow, have also been documented in the literature [8,14,15] (**Figure 2**). White adipose tissue (WAT) is comprised of adipocytes containing a single large lipid vesicle, which serves as a primary energy store in the body. In contrast, brown adipose tissue (BAT) consists of adipocytes with numerous small lipid droplets and primarily functions in thermoregulation.[16,17] Maintaining a harmonious balance of these two types of adipose tissue is essential for maintaining energy homeostasis in the body.[5,13]

Adipose tissue engineering is an expanding and demanding area of research, addressing current clinical needs for various adipose tissue pathologies and defects.[18] On one hand, research in WAT engineering focuses on producing soft tissue equivalents for plastic and reconstructive surgery.[7,19] On the other hand, BAT engineering is a relatively new research field aimed at replicating intricate thermogenic cell functions for *in vitro* or *in vivo* applications.[20]

BAT plays a crucial role in regulating body temperature through non-shivering thermogenesis.[21] This process is facilitated by brown adipocytes, which dissipate heat by uncoupling proton transport from ATP synthesis.[22] BAT is characterized by its abundant mitochondria and the presence of "uncoupling protein 1" (UCP1), enabling it to convert electrochemical energy generated during respiration into heat by uncoupling lipid oxidation in mitochondria.[23,24] Because of its significant impact on calorie expenditure, BAT is viewed as a promising therapeutic target in the fight against obesity.

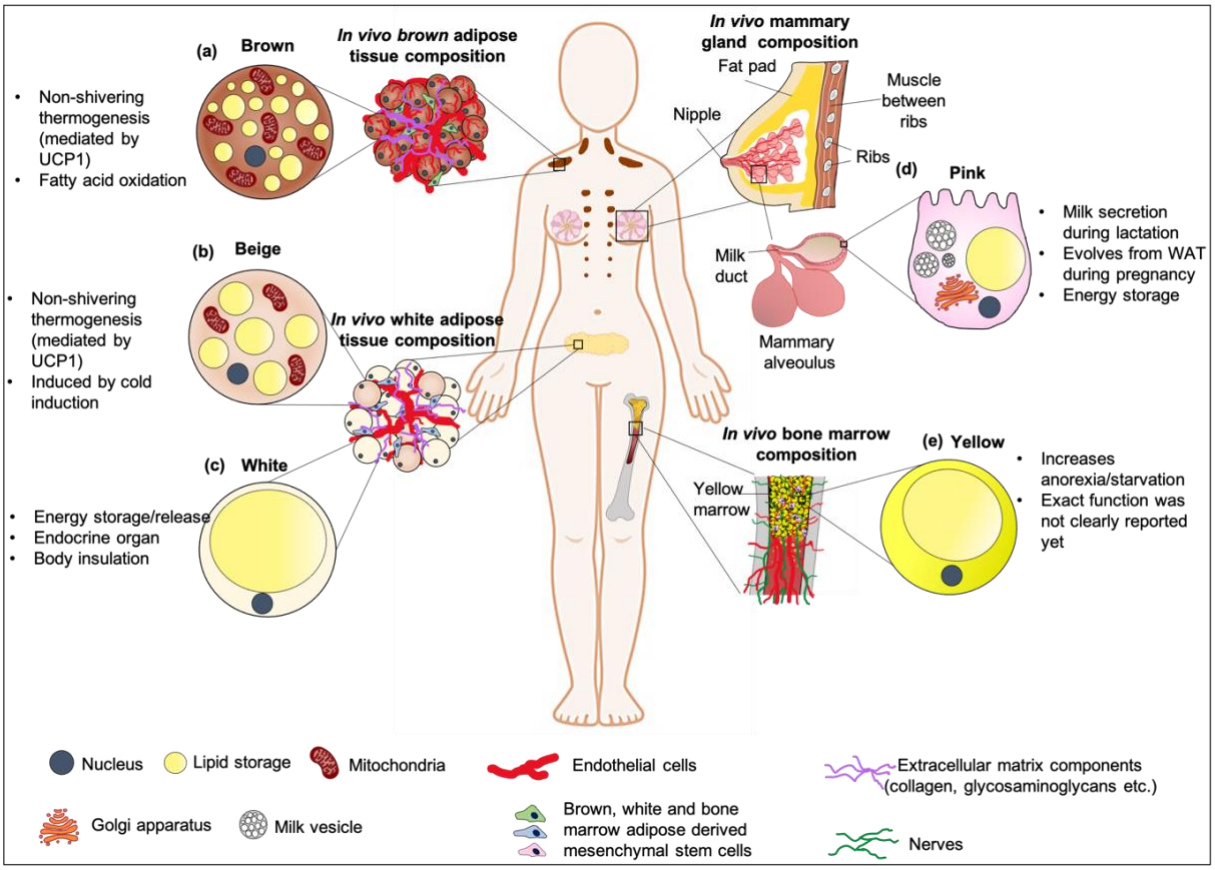


**Figure 2.** Adipose tissue types in the body. a) Brown adipocytes: Small lipid droplets, high UCP1 expression, thermoregulation in specific areas. b) Beige adipocytes: Found in white adipose tissue, adopt brown-like phenotype for thermoregulation. c) White adipocytes: Main cells in white adipose tissue, high energy storage, produce adipokines. d) Pink adipocytes: Secrete milk during pregnancy, reversible conversion from white adipocytes in mammary glands. e) Yellow adipocytes: Found in bone marrow, involved in systemic energy regulation.

Additionally, besides its role in regulating body temperature, adipose tissue displays remarkable plasticity and reprogramming capabilities. *In vitro*, mature white adipocytes can undergo reprogramming to transform into dedifferentiated fat (DFAT) cells, recognized as a novel type of stem cell.[25] DFAT cells exhibit high multipotency, demonstrating significant potential for redifferentiation into various lineages including osteogenic,[26,27] chondrogenic,[28] and adipogenic [29] pathways. This exceptional redifferentiation capacity, coupled with a straightforward isolation process,[25,30] positions DFATs as a valuable and abundant stem cell source applicable in tissue engineering, regenerative medicine, cell therapy, and stem cell research. Given these attributes, the reprogramming of mature white adipocytes into stem cells through dedifferentiation holds substantial promise for applications in BAT engineering and regenerative medicine.

The process of reprogramming mature white adipocytes through dedifferentiation relies on basically two different methods as shown in **Figure 3**. First, the ceiling culture technique as illustrated in **Figure 3A**, pioneered by Sugihara et al. in 1986. In this approach, cell culture flasks are completely filled with cell culture medium, allowing mature adipocytes to adhere to the upper surface of the flask.[31] Second method is glass cover slip method[30] illustrated in **Figure 3B**. Here, freshly isolated mature adipocytes are inserted into the multi-well plates and a glass cover slip placed on top to provide adipocyte attachment. Over the course of a few days, these adhered cells lose their lipid content, adopting a fibroblastic morphology, thereby yielding DFATs.

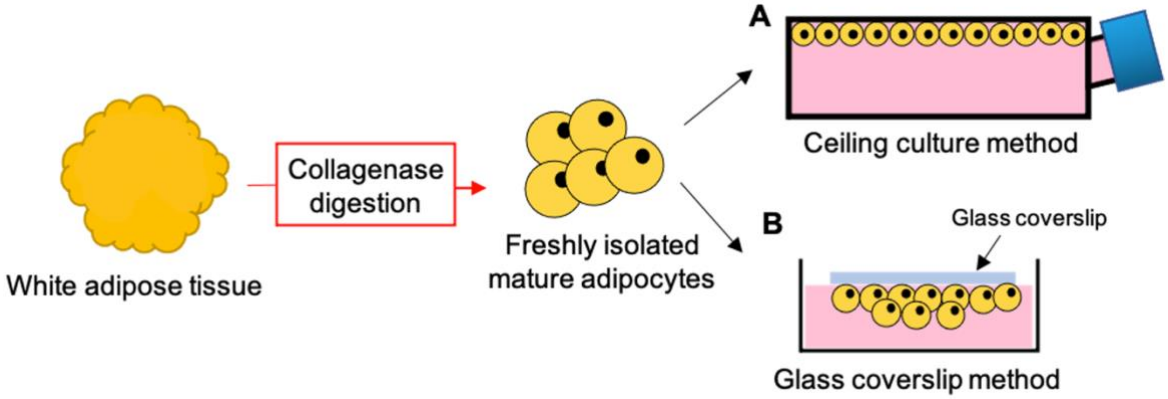


**Figure 3.** Methods for dedifferentiation of mature adipocytes. A) Ceiling culture method, B) glass cover slip method.

Upon comparing these two methods, the ceiling culture method is relatively more feasible and straightforward. Therefore, we have chosen the ceiling culture method for our study. While the ceiling culture method is straightforward, it is also time-intensive and demonstrates low efficiency. Our research indicates that only approximately 30% of initially seeded mature adipocytes undergo dedifferentiation using the traditional ceiling culture method. Consequently, our objective was to enhance and refine the dedifferentiation process of mature adipocytes by polymer coating the inner top layer of cell culture flasks.

The fundamental requirement for adipocyte dedifferentiation is cellular attachment. In this way, adipocytes lose their cytoplasmic fat and acquire stem cell properties with a fibroblastic morphology. To increase cellular attachment, the ceiling culture was improved by polymer coating with cationic polymers (PLL, PDDA, and PAH) and anionic polymers (Gel and GG), as well as key proteins found in the extracellular matrix (ECM) such as collagen type

I (Col 1) and fibronectin (Fib), and basement membrane (BM) components like collagen type IV (Col IV) and laminin (Lam).

Following the increase in DFAT yield through polymer coating, we proceeded to investigate the redifferentiation of these cells into brown adipocytes. While various scaffold materials have been explored to mimic native tissue environments and enhance biological functions of adipose tissue, there has been limited research on engineering thermogenic adipose tissue as a therapeutic approach for obesity-related diseases.[32–35] However, the specific influence of these added polymers on brown adipocyte redifferentiation has not been previously studied. To address this gap, brown adipose tissue-like structures were created by encapsulating DFATs in fibrin gel mixed with several biopolymers, including Col I, Col IV, Fib, Lam, Gel, GG, and PLL as a cationic polymer. Subsequently, the impact of polymer supplementation on browning within these developed structures was assessed.

For the third stage of the thesis, one highly efficient technique in tissue engineering to control the differentiation of DFAT into brown adipocytes may involve Layer-by-Layer (LbL) coating. LbL assemblies of nanofilms entail constructing ultra-thin coatings by sequentially assembling materials or cells layer by layer. These coatings can be applied to cells using interactions such as electrostatic, hydrophobic, and biological recognition mechanisms. [36–38] LbL film assemblies have demonstrated significant potential in guiding cell behavior, enhancing adhesion, migration, and proliferation, as well as activating signaling pathways.[39–43] Consequently, they play a crucial role in regulating cell functions like differentiation.[44,45] Moreover, this method is rapid, versatile, and cost-effective for modifying surface properties. Importantly, there have been no previous reports on the differentiation of stem cells coated with polyelectrolyte nanofilms into brown adipocytes.

As a result, the main purposes of this thesis are summarized in **Figure 4**. In Step 1, white adipocytes were dedifferentiated to obtain DFATs. Then, in Step 2, these DFATs were redifferentiated into brown adipocytes.

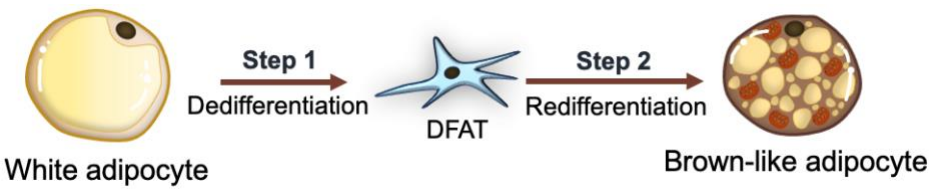


**Figure 4.** Main purpose of thesis by following two step strategy.

**Outline of this thesis**

In this thesis, the author describes the fabrication of BAT by following a two-step strategy and controlling the cell microenvironment with polymers. This thesis is organized into the following three chapters.

**Chapter 1**

**ECM Proteins and Cationic Polymers Coating Promote Dedifferentiation of Patient-Derived Mature Adipocytes to Stem Cells**

To effectively control the dedifferentiation ratio of mature white adipocytes, it is advantageous to coat the inner top layer of the cell culture flask with specific polymers and proteins. This method aims to enhance the adherence of mature white adipocytes to the substrate surface, a crucial factor for successful dedifferentiation. The focus of this chapter was on optimizing this adherence process. After applying the coatings, we evaluated the physicochemical properties of the substrate surface, such as hydrophobicity and electrostatic interactions. These properties were then analyzed to understand their influence on the dedifferentiation efficiency and the resulting DFAT ratio. By systematically examining these parameters, we aimed to establish a more effective protocol for promoting the dedifferentiation of mature white adipocytes.

**Chapter 2**

**Cationic Polymer Effect on Brown Adipogenic Induction of Dedifferentiated Fat Cells**

The influence of local factors on the fate of stem cells is intricate, with external factors such as polymers playing a significant role in affecting vital cellular processes like differentiation. Furthermore, the differentiation of adipocytes involves a well-coordinated interaction between external stimuli and an intricate network of receptors and transcription factors within the nucleus. In this chapter, our objective was to assess the impact of different polymers, including Col I, Fib, Lam, Gel, GG, and PLL, on the *in vitro* brown adipogenic redifferentiation of DFATs encapsulated within a fibrin gel. This evaluation aimed to shed light on how these various polymers can influence and potentially enhance the differentiation process towards brown adipocytes, thereby contributing to advancements in tissue engineering and regenerative medicine.

## Chapter 3

## Polyelectrolyte Nanofilms on Cell Surface Can Induce Brown Adipogenic Differentiation of DFATs

In the previous chapter, we identified that polycations, especially PLL, significantly enhance brown adipogenesis during the 3D differentiation of DFATs within fibrin gels. However, the differentiation was inhomogeneous due to uncontrolled attachment of PLL and DFATs within the gels. To address this issue, this chapter explores the application of polyelectrolyte (PE) nanofilms, specifically composed of PLL and dextran sulfate (DES), directly onto the surfaces of DFATs. By coating DFATs with three layers of these PE nanofilms and encapsulating them in fibrin gel, we achieved a more uniform differentiation process. The brown adipogenic differentiation status of the nanofilm-coated DFATs was then assessed using immunofluorescence and gene expression analyses. This strategy aimed to improve the consistency and efficiency of DFAT differentiation into brown adipocytes, paving the way for more reliable applications in tissue engineering and regenerative medicine.

## References


1. F. Akter, in *Tissue Engineering Made Easy*, Academic Press **2016**, 1.
2. J. Velema and D. Kaplan, *Tissue Engineering I* **2006**, 187.
3. R. Langer and J. P. Vacanti, *Science* **1993**, *260*, 920.
4. M. Anand, M. Bhagania and K. Kaur, *Archives of Aesthetic Plastic Surgery* **2023**, *29*, 64.
5. J. H. Choi, J. M. Gimble, K. Lee, K. G. Marra, J. P. Rubin, J. J. Yoo, G. Vunjak-Novakovic and D. L. Kaplan, *Tissue Eng. Part B Rev.* **2010**, *16*, 413.
6. C. Conci, L. Bennati, C. Bregoli, F. Buccino, F. Danielli, M. Gallan, E. Gjini and M. T. Raimondi, *J. Tissue Eng. Regen. Med*. **2020**, *14*, 369.
7. P. Kamat, F. S. Frueh, M. McLuckie, N. Sanchez-Macedo, P. Wolint, N. Lindenblatt, J. A. Plock, M. Calcagni and J. Buschmann, *Cytotherapy* **2020**, *22*, 400.
8. F. Louis and M. Matsusaki, *Biomater. Organ Tissue Regener*. Woodhead Publishing, **2020**, 393.
9. S. Miettinen, J. R. Sarkanen and N. Ashammakhi, *Topics in Tissue Engineering* **2008**, 1.
10. E. C. M. Mariman and P. Wang, *Cell Mol. Life Sci.* **2010**, *67*, 1277.
11. E. D. Rosen and O. A. MacDougald, *Nat. Rev. Mol. Cell Biol.* **2006**, *7*, 885.
12. L. Z. Sharp, K. Shinoda, H. Ohno, D. W. Scheel, E. Tomoda, L. Ruiz, H. Hu, L. Wang, Z. Pavlova, V. Gilsanz and S. Kajimura, *PLoS One* **2012**, 7, e49452.
13. M. Esteve Ràfols, *Endocrinología y Nutrición (Engl. Ed.)* **2014**, *61*, 100.
14. S. Cinti, *Nutr. Metab. Cardiovasc. Dis.* **2006**, *16*, 569.
15. K. Aubin, M. Safoine, M. Proulx, M. A. Audet-Casgrain, J. F. Côté, F. A. Têtu, A. Roy and J. Fradette, *PLoS One*, **2015**, *10*, 1.
16. B. Cannon and J. Nedergaard, *Physiol Rev*, 2004, **84**, 277–359.
17. A. M. Cypess, S. Lehman, G. Williams, I. Tal, D. Rodman, A. B. Goldfine, F. C. Kuo, E. L. Palmer, Y. H. Tseng, A. Doria, G. M. Kolodny and C. Ronald Kahn, *Obstet. Gynecol. Surv*. **2009**, *64*, 519.
18. E. Donnely, M. Griffin and P. E. Butler, *Ann. Biomed. Eng.* **2020**, *48*, 9.
19. M. V. Plikus, C. F. Guerrero-Juarez, M. Ito, *Science* **2017**, *355*, 748.
20. A. M. Unser, Y. Tian and Y. Xie, *Biotechnol. Adv*. **2015**, *33*, 962.
21. A. Smorlesi, A. Frontini, A. Giordano and S. Cinti, *Obesity Reviews*, **2012**, *13*, 83.
22. D. F. Pisani, V. Barquissau, J. C. Chambard, D. Beuzelin, R. A. Ghandour, M. Giroud, A. Mairal, S. Pagnotta, S. Cinti, D. Langin and E. Z. Amri, *Mol Metab*. **2018**, *7*, 35.
23. E. T. Chouchani, L. Kazak and B. M. Spiegelman, *Cell Metab.* **2019**, *29*, 27.
24. M. Christian, *Handb. Exp. Pharmacol*. **2019**, *251*, 85.
25. M. Jumabay, *World J. Stem Cells* **2015**, *7*, 1202.
26. T. Yanagi, H. Kajiya, S. Fujisaki, M. Maeshiba, A. Yanagi-S, N. Yamamoto-M, K. Kakura, H. Kido and J. Ohno, *Regen Ther*. **2021**, *18*, 472.

27. T. Kazama, M. Fujie, T. Endo and K. Kano, *Biochem. Biophys. Res. Commun*. **200**8, *377*, 780.
28. M. Shimizu, T. Matsumoto, S. Kikuta, M. Ohtaki, K. Kano, H. Taniguchi, S. Saito, M. Nagaoka and Y. Tokuhashi, *J. Orthop. Sci.* **2018**, *23*, 688.
29. X. Hu, P. Luo, X. Peng, T. Song, Y. Zhou, H. Wei, J. Peng and S. Jiang, *Gen. Comp. Endocrinol.* **2015**, *214*, 77.
30. J. Lessard, J. A. Côté, M. Lapointe, M. Pelletier, M. Nadeau, S. Marceau, L. Biertho and A. Tchernof, *JOVE*, **2015**, *97*, 52485.
31. H. Sugihara, N. Yonemitsu, S. Miyabara and K. Yun, *Differentiation* **1986**, *986*, 42.
32. K. M. Tharp, A. K. Jha, J. Kraiczy, A. Yesian, G. Karateev, R. Sinisi, E. A. Dubikovskaya, K. E. Healy and A. Stahl, *Diabetes* **2015**, *64*, 3713.
33. M. K. Vaicik, M. Morse, A. Blagajcevic, J. Rios, J. C. Larson, F. Yang, R. N. Cohen, G. Papavasiliou and E. M. Brey, *J. Mate.r Chem. B* **2015**, *3*, 7903.
34. J. P. Yang, A. E. Anderson, A. McCartney, X. Ory, G. Ma, E. Pappalardo, J. Bader and J. H. Elisseeff, *Tissue Eng. Part A* **2017**, *23*, 253.
35. J. H. Hammel and E. Bellas, *Integr. Biol. (Camb.)* **2020**, *12*, 81.
36. M. Matsusaki, H. Ajiro, T. Kida, T. Serizawa and M. Akashi, *Adv. Mater.* **2012**, *24*, 454.
37. K. Kadowaki, M. Matsusaki and M. Akashi, *Chem. Lett.* **2012**, *5*, 523.
38. J. Zeng and M. Matsusaki, *Polym. Chem.* **2019**, *10*, 2960.
39. U. Han, Y. J. Kim, W. Kim, J. H. Park and J. Hong, *Nanoscale* **2019***, 11,* 13541.
40. B. K. Ekambaram, M. S. Niepel, B. Fuhrmann, G. Schmidt and T. Groth, *ACS Biomater. Sci. Eng*. **2018**, *4*, 1820.
41. F. Han, P. Zhang, X. Wen, C. Lin and P. Zhao, *Biomater. Sci*. **2019**, *7*, 4388.
42. F. Gaudière, I. Masson, S. Morin-Grognet, O. Thoumire, J. P. Vannier, H. Atmani, G. Ladam and B. Labat, *Soft Matter.* **2012**, *8*, 8327.
43. M. S. Niepel, B. K. Ekambaram, C. E. H. Schmelzer and T. Groth, *Nanoscale*, **2019**, *11*, 2878.
44. D. Choi, J. Heo and J. Hong, *Langmuir* **2021**, *37*, 4587.
45. J. Hwang, D. Choi, M. Choi, Y. Seo, J. Son, J. Hong and J. Choi, *ACS Appl. Mater. Interfaces* **2018***, 10,* 17685.

# Chapter 1

## ECM Proteins and Cationic Polymers Coating Promote Dedifferentiation of Patient-Derived Mature Adipocytes to Stem Cells

## 1.1 Introduction

Adipose tissue and adipocytes have been extensively studied due to their role in obesity and related health issues. Adipose tissue, constituting 10-30% of body weight, regulates body homeostasis through endocrine and secretory functions that influence insulin sensitivity, lipid metabolism, and satiety.[1–3] Mature adipocytes, the primary cells in adipose tissue, can expand to 290 microns and are surrounded by preadipocytes, nerves, and capillaries in a honeycomb-like arrangement.[4] These cells exhibit high plasticity and can reprogram themselves in response to various cues, making them unique.[5] They can also dedifferentiate into stem cells called as DFATs, losing their lipid content and acquiring multipotent properties, with a spindle-shaped morphology.[6] DFATs can redifferentiate into multiple cell types and are more readily available than other stem cells, making them valuable for tissue engineering, regenerative medicine, and cell therapy.

DFATs can redifferentiate into various lineages, including osteogenic, chondrogenic, and adipogenic lineages, similar to stromal vascular fraction cells.[7,8] They have been shown to redifferentiate into peripheral nerve,[9] skeletal muscle,[10] cartilage,[11] bone,[12] and fat[13] cells *in vitro.* However, culturing mature adipocytes is challenging due to their high lipid content and buoyancy, which prevent them from adhering to the bottom of culture dishes using traditional methods.[4] Various culture techniques, such as ceiling culture and coverslip methods, have been developed to overcome these challenges and promote dedifferentiation. In ceiling culture, flasks are fully filled with cell culture medium, allowing adipocytes to attach to the flask ceiling, lose their lipid content, and gain fibroblastic appearance.[14] In another method, coverslips are used to facilitate cell adhesion and dedifferentiation.[15,16] Studies have shown that the YAP/TAZ, Hippo, Hedgehog, and PPARγ signaling pathways, which reorganize the cytoskeleton, play a role in this process.[17,18] Based on this finding, first, we focused on enhancing cell adhesion and dedifferentiation through the interaction of integrin molecules, which facilitate cell attachment to surfaces, as well as ECM and BM components. Second, we aimed to increase the adsorption

of vitronectin and fibronectin proteins, recognized as cell adhesion factors in serum[19,20] on the surface of cell culture flasks. This was achieved by coating the flask surfaces with positively charged polymers to improve cell adhesion and subsequently dedifferentiation. Finally, we validated the effect of cationic polymers on increasing DFAT by also coating cell culture flasks with anionic polymers.

## 1.2 Experiments

### 1.2.1 Materials

Collagen type IV (from human placenta, C7521), Fibronectin (from human plasma, F2006), Poly-L-lysin (PLL, P4707), Poly(allylamine) (PAH, 479136), Poly(diallyl dimethylammonium chloride) (PDDA, 26062-79-3), Collagenase (from Clostridium histolyticum, type I, C0130), Triton-X 100 (T8787), Collagen type I-FITC conjugated from bovine skin (C4361), Poly-L-lysine-FITC conjugated (P3543), CD90 (Anti-THY1) primary antibody (HPA003733), and Bovine Serum Albumin (BSA, 3294), Alcian Blue 8GX solution (1003580143) and Oil Red O (O06625) were purchased from Sigma-Aldrich (St Louis, MO, USA). Collagen type IV-FAM conjugated (AS-85112) obtained from AnaSpec (California, USA). Rhodamine Laminin (LMN01-A), and Rhodamine Fibronectin (FNR01-A) obtained from Cytoskeleton, Inc. (Denver, USA), YAP primary antibody (sc-101199) obtained from Santa Cruz (Texas, USA). Hoechst 33324 (H3570), Trypan Blue (T10282), Pierce™ BCA protein assay kit (23225), were purchased from ThermoFisher Scientific (Whaltam, MA, USA), Invitrogen. Phosphate Buffer Saline (D-PBS, 14249-24) and Dulbecco's Modified Eagle Medium (DMEM) high glucose (08458-16) came from Nacalai Tesque Inc. (Kyoto, Japan). Fetal Bovine Serum (FBS, 10270106) was obtained from Gibco. Phalloidin-iFlour 594 Reagent (ab176757) Trypsin (207192-83), Gelatin (077-03155) and Alizarin Red S (011-01192) came from Wako Pure Chemical Industries (Tokyo, Japan). Live/Dead® viability assay kit (PK-CA707-30002) purchased from PromoKine (Heidelberg, Germany), T12.5 cell culture flasks (353018) and Laminin (354259) obtained from Corning (Arizona, USA). Collagen type I (from bovine dermis, Atelocell, IPC-50) from Koken (Tokyo, Japan). Gellan Gum (8H1121A) came from Sansho (Osaka, Japan). APC anti human CD105 (323207), APC anti-human CD90 (328113), APC anti-human CD73 (344005), APC/Cyanine7 Mouse IgG2b, κ Isotype Ctrl (402210) purchased from BioLegend (San Diego, California, USA). APC anti human CD44 (560532) obtained from BD Biosciences (New Jersey, USA).

### 1.2.2 Isolation of mature adipocytes

Human adipose tissue samples were collected from patients at Kyoto University Hospital. Prior to adipocyte isolation, the tissues were washed with PBS containing 5% antibiotics. Then, 2-3 grams of adipose tissue were placed into each well of a 6-well plate and minced into approximately 1 $mm^3$ pieces using autoclaved tweezers and scissors. Each well received 2 mL of collagenase solution (2 mg/mL in DMEM with 0% FBS, 5% BSA, and 1% antibiotics, sterilized by filtration) and was incubated on shaking incubator for 1 hour at 37°C with a rotation speed of 250 rpm. Following incubation, the lysate was filtered using a 500 µm pore size filter and centrifuged for 3 minutes at 80g. After centrifugation, mature adipocytes were found floating at the top of the tube, while stromal vascular fractions (SVFs) settled at the bottom. The liquid between the top layer and the pellet was removed using a 10 mL pipette, and the washing process was repeated twice with PBS containing 5% BSA and 1% antibiotics, with a final wash in DMEM. Freshly isolated mature adipocytes were used for all ceiling culture experiments.

**Ethics statement:** Adipose tissues were collected from Kyoto University Hospital (Kyoto, Japan) following abdominal adipose tissue or liposuction procedures from three human donors aged 41, 45, and 53 years, with body mass indices (BMI) of 22.40, 25.78, and 20.46, respectively. All procedures were approved by the Osaka University Research Ethics Review Committee (approval number: L026).

### 1.2.3 Polymer and protein coating on cell culture flasks

A collagen type I solution (AteloCell IPC50, 5 mg/mL) was diluted to 125 µg/mL with PBS (pH 7.4). Collagen type IV and fibronectin solutions were prepared at 125 µg/mL and 62.5 µg/mL in PBS (pH 7.4), respectively. To dissolve collagen type IV, the stock solution was refrigerated at 4°C. Polystyrene (PS) cell culture flasks (12.5 $cm^2$) were coated with 10 µg/$cm^2$ of collagen type I and IV and 5 µg/$cm^2$ of fibronectin for 1 hour at room temperature, following recommended protocols. A laminin solution was prepared at 12.5 µg/mL in PBS (pH 7.4) on ice and used to coat PS flasks at 1 µg/$cm^2$ at 4°C overnight. For cationic (PLL, PDDA, PAH) and anionic (gelatin, gellan gum) polymers, PS flasks were coated with 8.33 µg/$cm^2$ of polymer in sterile aqueous solutions for 5 minutes at room temperature, following the provider's protocol. After incubation, flasks were washed three times with PBS (pH 7.4). All coating procedures were conducted in a laminar flow hood to minimize contamination.

### 1.2.4 Ceiling culture with coated cell culture flasks

Freshly isolated mature adipocytes were seeded at a density of $5.0\times10^4$ cells/cm² in protein and polymer coated PS flasks, which were then completely filled with DMEM containing 20% FBS and 1% antibiotics. The schematic illustration of the method shown in **Figure 1-1**. The flasks were tightly capped to prevent medium leakage and incubated at 37°C for one week. After incubation, the medium was aspirated, and the obtained DFATs were detached via trypsinization. The cells were counted using an automated cell counter (Invitrogen) with Trypan Blue. To normalize the data, the DFAT count from uncoated surfaces was used as a control to compare cell numbers under different conditions.

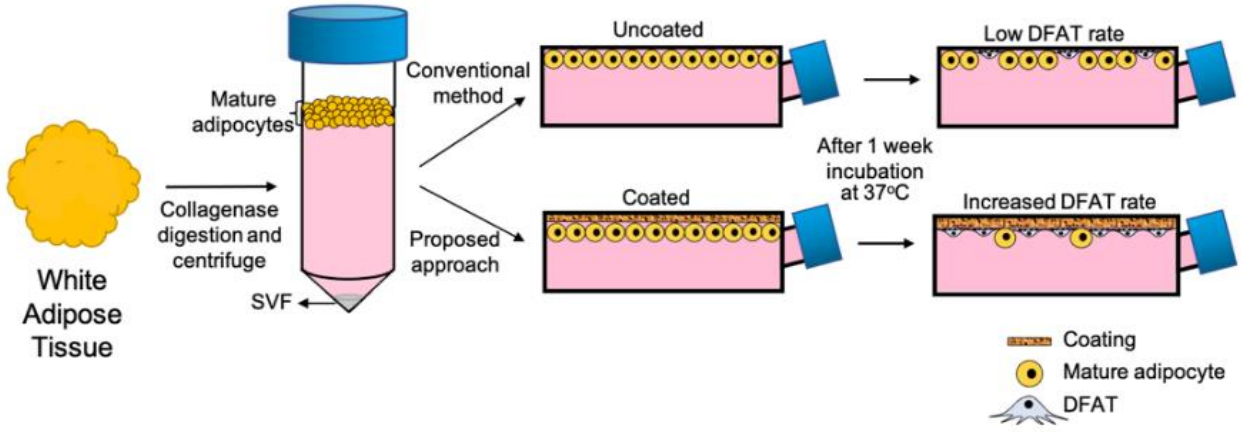


**Figure 1-1.** Schematic illustration of improved ceiling culture method to increase DFAT cell rate by extracellular matrix, basement membrane and cationic/anionic polymer coating on the inner top surface of the cell culture flasks.

### 1.2.5 Water contact angle measurements

Contact angles of protein and polymer coated PS surfaces were measured using the sessile drop method (n=3). PS microscope slides (2.5×7.5 cm²) served as substrates for wettability measurements and were coated under the same conditions as the PS cell culture flasks. A 19 G micro syringe was used to place 5 µL Milli-Q water droplets on the surface, and photographs were taken at the moment of contact. The images were then analyzed using FAMAS software with a Kyowa Contact Angle meter.

### 1.2.6 Zeta potential measurements of coating solutions

The zeta potential of protein and polymer solutions was determined using a Malvern ZetaSizer. Disposable folded capillary cells were filled with 800 µL of coating solutions prepared in PBS (pH 7.4), and measurements were performed using dynamic light scattering at 25°C (n=3).

### 1.2.7 Adsorbed protein assessment on cationic polymer coated surfaces

To evaluate the amount of serum protein adsorbed on PS surfaces coated with cationic polymers (PLL, PDDA, PAH), 96-well plates were coated with these polymers at a concentration of 8.33 µg/cm² for 5 minutes at room temperature. To assess the amount of serum protein adsorbed on coated PS plates, 25 µL of DMEM high glucose (containing 20% FBS and 1% antibiotic) was added to 96-well plates. The plates were then incubated at 37°C for 0.5, 1, 3 and 16 hours. The total adsorbed protein in each well was quantified using a bicinchoninic acid (BCA) assay. After incubation, the medium was removed, and 200 µL of BCA working solution was added to each well, followed by a 30-minute incubation at 37°C. The optical density was measured at 562 nm using a microplate reader and compared to a standard curve prepared with BSA as the standard protein.

### 1.2.8 Fluorescence labeled polymer and protein coating on cell culture dishes

Fluorescently labeled protein and polymer solutions were prepared in PBS (pH 7.4) and coated onto PS cell culture flasks under identical conditions. FITC-conjugated collagen type I, FAM-conjugated collagen type IV, rhodamine-labeled laminin, rhodamine-labeled fibronectin, and FITC-conjugated PLL were applied to 96-well plates at concentrations of 10 µg/cm², 10 µg/cm², 1 µg/cm², 5 µg/cm², and 8.33 µg/cm², respectively, mirroring the coating concentrations used on the PS cell culture flasks. Following protein and polymer coating, the wells were washed three times with PBS (pH 7.4) and imaged using an FV3000 Confocal Laser Scanning Microscope (Olympus, Tokyo, Japan). Image J software (Fiji, Mac OS X version) was utilized for fluorescence intensity analysis of each coated surface.

### 1.2.9 Characterization of DFATs

***Immunofluorescence imaging of DFATs:*** After 1 week of ceiling culture in uncoated PS flasks, DFATs were transferred to 10 cm Petri dishes and cultured until reaching 80% confluence. They were then reseeded onto 96-well plates at $1.2 \times 10^4$ cells per well. Upon reaching confluence, cells were fixed overnight at 4°C in 4% paraformaldehyde/PBS, permeabilized with 0.05% Triton X-100/PBS for 15 minutes, and blocked with 1% BSA/PBS for 1 hour at room temperature. Anti-CD90 and anti-YAP antibodies were applied in 1% BSA/PBS and incubated overnight at 4°C. The following day, samples were incubated with secondary antibodies (Alexa Fluor 647 and Alexa Fluor 488) for 2 hours at room temperature in the dark. For Oct-4 staining, DFATs were incubated with primary antibody (MA1-104, Thermo Fisher) for 1 hour at room temperature, followed by incubation with Alexa Fluor 488 secondary antibody for 2 hours in the dark. Finally, cells were stained for F-actin using CytoPainter Phalloidin-iFluor 594 and nuclei were counterstained with Hoechst. After washing with PBS, samples were imaged using an FV3000 Confocal Laser Scanning Microscope (Olympus, Tokyo, Japan).

***Multilineage differentiation of DFATs:*** DFATs were differentiated into osteoblasts, chondrocytes, and adipocytes by seeding in 24-well plates at $5.0 \times 10^3$ cells per well for osteogenic and chondrogenic differentiation using StemPro kits as per manufacturer's instructions. For adipogenic differentiation, cells were seeded at $1.2 \times 10^4$ cells per well in Adipocyte Differentiation Medium (Cell Applications, Inc.). Alizarin Red S staining on day 21 confirmed osteogenic differentiation, Alcian Blue staining on day 14 confirmed chondrogenic differentiation, and Oil Red O staining on day 14 confirmed adipogenic differentiation.

***Flowcytometry analysis of DFATs:*** To characterize DFATs, flow cytometry was performed. Cells were detached with trypsin/EDTA and incubated on ice for 30 minutes in PBS with 10% FBS. After centrifugation at 3500 rpm for 1 minute, at least $2.5 \times 10^5$ cells per Eppendorf tube were incubated with APC-conjugated antibodies against CD44, CD73, CD90, and CD105, or the respective isotype control (1/50 in 1% BSA in PBS) on ice for 45 minutes in the dark. Following washing, labeled cells were analyzed using a BD FACSMelody flow cytometer and FlowJo software.

***Statistical Analysis*:** In this study, three independent experiments were conducted for each test, and results are presented as means ± SD. Error bars indicate standard deviations. Statistical analysis was performed using Student's *t*-test, with *p* values considered significant at $*p < 0.05$.

## 1.3. Results and discussion

### 1.3.1 Hydrophobicity effect assessment of DFAT ratio

In this study, we investigated the relationship between the physicochemical surface properties of coated PS surfaces and the resulting DFAT ratio. Specifically, we focused on hydrophobicity or water wettability, which is a crucial surface property influencing cell adhesion, proliferation, and interaction.[21]

To evaluate wettability, PS surfaces were coated with proteins and polymers, and water contact angle (C.A.) measurements were taken. Images of water C.A. for protein, cationic, and anionic polymer-coated surfaces are shown in **Figure 1-2A, D**, and **G**, respectively, with values in **Figure 1-2B, E**, and **H** (gray bars). DFAT cells obtained from these surfaces after 1 week of culture were also measured (red bars). The C.A. of uncoated PS was 82° (± 2.6). For protein-coated PS, C.A. values were 73° (± 5.4) for laminin, 54° (± 2.9) for fibronectin, and 39° (± 6.0) and 39° (± 3.6) for collagen type IV and type I, respectively (**Figure 1-2A, B**). DFAT ratios were highest for laminin and collagen type I surfaces, with values of 2.98 (± 0.92) and 2.89 (± 0.84), respectively, while fibronectin and collagen type IV surfaces had ratios of 1.84 (± 0.43) and 2.41 (± 0.83) **(Figure 1-2B**, red bars).

A surface is considered hydrophobic if the C.A. value is between 150° and 90°, super hydrophobic if above 150°, hydrophilic if between 90° and 10°, and super hydrophilic if below 10°.[21] Moderate hydrophobicity around 70° is generally accepted as favorable for cell adhesion and spreading.[22,23]

The C.A. values of ECM and BM protein-coated surfaces, ranging from 54° to 73°, are suitable for cell adhesion and dedifferentiation of mature adipocytes. For cationic polymer-coated PS surfaces, C.A. values were 79° (PAH), 80° (PLL), and 91° (PDDA). Despite higher C.A. values, PLL and PDDA showed higher DFAT ratios than PAH. PAH had a DFAT ratio of 1.27, while PLL and PDDA had ratios of 2.19 and 2.27, respectively. This suggests that cationic polymer coatings may affect DFAT ratios, through different mechanism such as electrostatic

interactions not just hydrophobicity.

For anionic polymer-coated surfaces, the C.A. values were 65° for Gel and 90° for GG. These coatings resulted in lower DFAT ratios of 0.85 and 0.32, respectively. This indicates that proteins and cationic polymers positively affect cell attachment compared to anionic polymers, suggesting other mechanisms besides hydrophobicity may influence the DFAT ratio in charged polymer coatings.

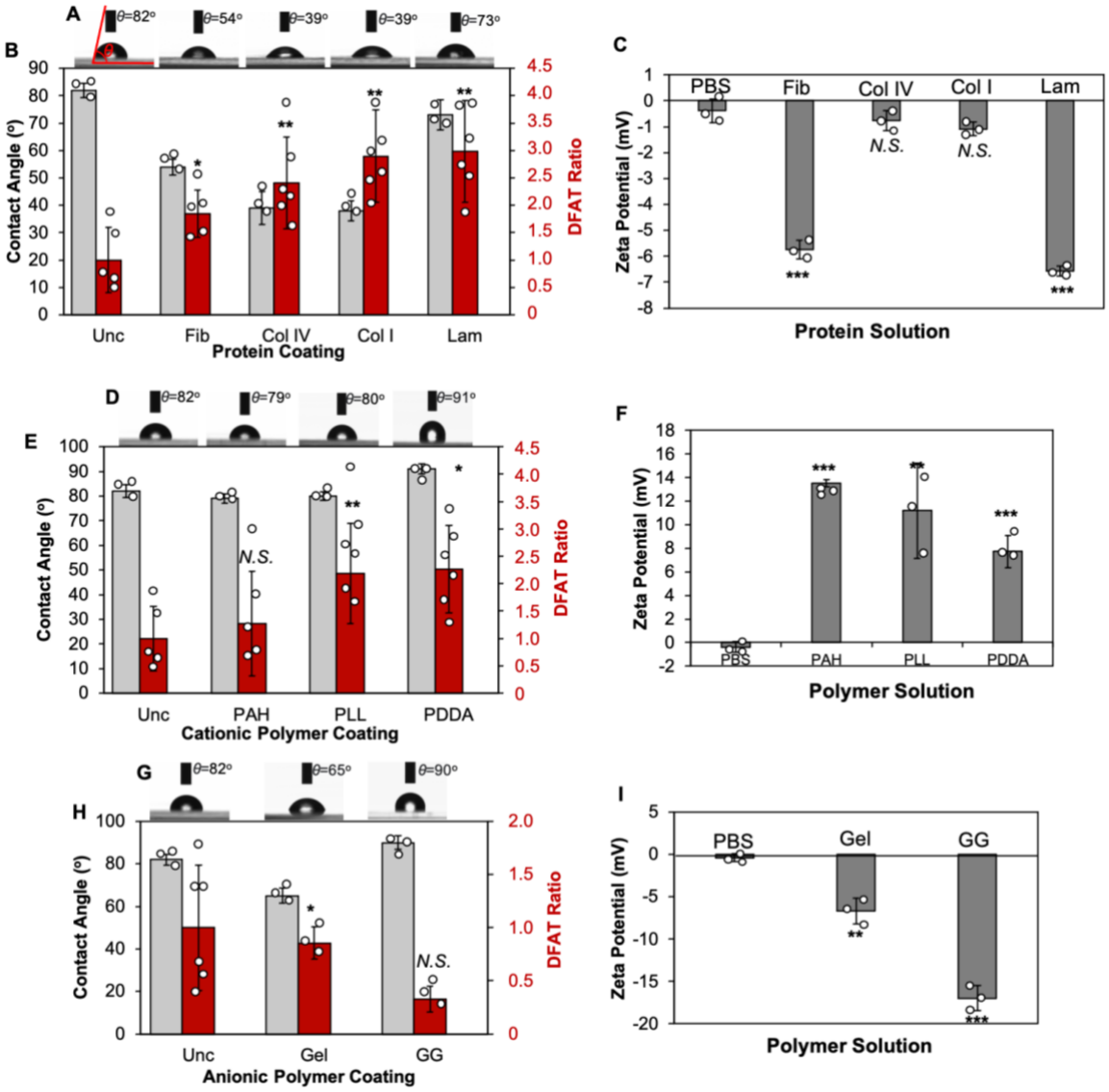


**Figure 1-2.** A) Coating effect assessment of DFAT rate. Contact angle images of protein coated (A), cationic polymer coated (D) and anionic polymer coated (G) surfaces by sessile drop method performed on n=3. Contact angle values after coating (grey bars) and obtained DFAT cell numbers 1 week of ceiling culture with 20% FBS (v/v) included DMEM high glucose on protein coated (B), cationic polymer (E) and anionic polymer (H) coated surfaces (red bars). To normalize the data, obtained DFAT cell number by uncoated surface used as control to compare the other conditions obtained DFAT cell number. Statistically significant differences are stated

by symbols: *$p$<0.1, **$p$<0.01, and ***$p$<0.001 when the control group is DFAT ratio from uncoated PS surface. The graphs show results as means ± s.d. of experiments performed on n=6. Zeta potential measurements of protein (C), cationic polymer (F) and anionic polymer (I) solutions for coating. Statistically significant differences are stated by symbols: *$p$<0.01, **$p$<0.001 and, ***$p$<0.0001 when the control group is PBS (pH:7.4) (*N.S.*: Not significant). The graphs show results as means ± s.d. of experiments performed on n=3.

### 1.3.2 Electrostatic effect assessment on DFAT ratio

Mammalian cell membranes typically exhibit a negative surface charge at pH 7, approximately -19.4 (± 0.8) mV for HeLa cells and -31.8 (± 1.1) mV for erythrocytes.[24] Therefore, cells are attracted to positively charged surfaces and repelled by negatively charged ones. The increase in DFAT ratio with cationic polymer coating is likely facilitated by enhanced cellular attachment through electrostatic interactions. However, the mechanism by which ECM and BM proteins increase the DFAT ratio is probably related to biological processes such as integrin interactions and actin myofibril reorganization, rather than purely electrostatic interactions.

PLL, PDDA, and PAH enhanced the DFAT ratio by 2.19 (± 0.91), 2.27 (± 0.8), and 1.27 (± 0.95) times, respectively (**Figure 1-2E**, red bars). Despite PAH exhibiting the highest zeta potential, its effect on increasing the DFAT ratio was less pronounced compared to PLL and PDDA. This discrepancy might be attributed to higher potential of cytotoxicity associated with PAH in cell culture.[25]

Cationic polymer-coated surfaces are hypothesized to facilitate the adsorption of serum proteins despite having a slightly negative zeta potential, contrasting with anionic polymers that support cell attachment and dedifferentiation. We conducted an experiment where surfaces were exposed to DMEM containing 20% FBS for durations of 0.5, 1, 3, and 16 hours, followed by a BCA assay to quantify the levels of adsorbed proteins (**Figure 1-3**). It is likely that positively charged polymers like PDDA and PLL enhance cell adhesion by increasing the adsorption of serum proteins, thereby potentially elevating the DFAT ratio. In the context of ceiling culture on PS surfaces coated with anionic polymers, such as gelatin and gellan gum solutions (**Figure 1-2I**), zeta potential measurements revealed values of -6.67 (± 0.51) and -6.96 (± 1.45) mV, respectively. The resulting DFAT ratios were 0.86 (± 0.15) for gelatin and 0.33 (± 0.12) for gellan gum (**Figure 1-2H**, red bars). These negatively charged surfaces are likely to hinder cell

attachment and dedifferentiation by reducing the adsorption and interaction of positively charged serum proteins and cells.

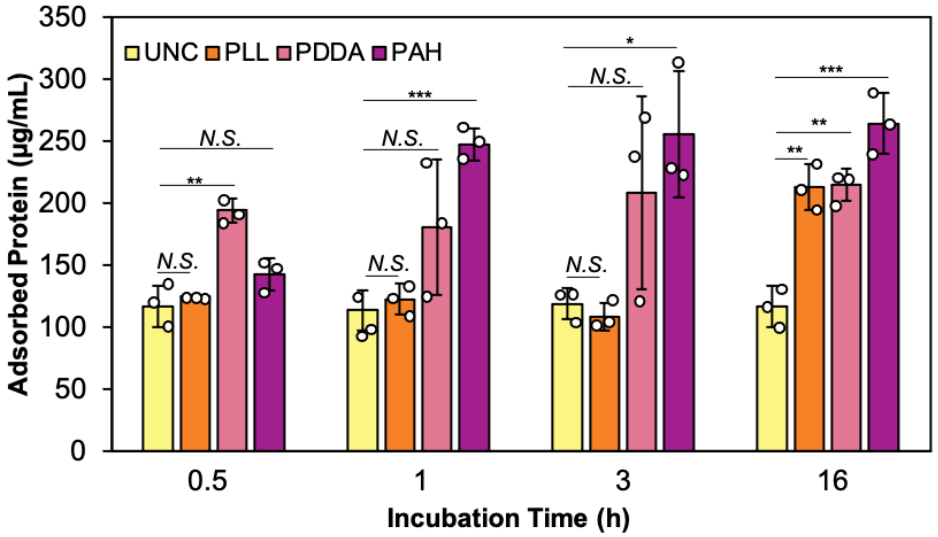


**Figure 1-3.** The level of adsorbed protein from 20% FBS (v/v) in DMEM high glucose incubation was assessed on cationic polymer-coated surfaces at various time points (n=3). Statistically significant differences are denoted by symbols: *$p$<0.01, **$p$<0.001, *N.S.* for not significant.

### 1.3.3 Proteins and polymers amount effect assessment on DFAT ratio

Another possible explanation for the different impacts of proteins and polymers on DFAT ratio might be the amount that remains on the surface after coating. To examine this, PS surfaces were coated with polymers and proteins that were labeled with fluorescence (**Figure 1-4A**). Confocal microscope images were captured, and Image J was used to measure the fluorescence intensity (F.I.) of the surfaces, confirming the presence of the respective coatings (**Figure 1-4B**). No fluorescence was observed on uncoated surfaces, as expected. The F.I. values measured were 35.4, 21.4, 18.1, 30.9, and 23.1 (xE+0.6) for Fib, Col IV, Col I, Lam, and PLL, respectively, on day 7. However, F.I. could not be detected on PS surfaces coated with anionic polymers, likely due to their possible thin coating. Despite this, these polymers might still influence FBS protein adsorption and cell attachment. Although the F.I. method lacks high sensitivity, it suggests that these polymers are present on the surface, albeit at a molecular level. Therefore, anionic polymer coating appears to impact the DFAT ratio, potentially by inhibiting FBS protein adsorption or limiting cell attachment.

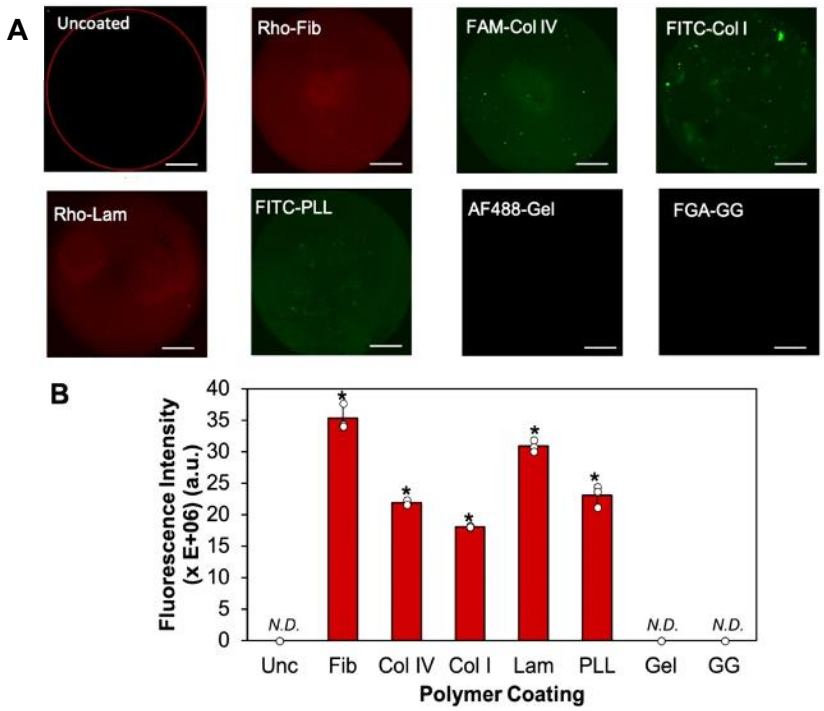


**Figure 1-4.** Fluorescently labeled polymer coatings were applied to tissue culture polystyrene well plates. A) Confocal laser scanning microscopy (CLSM) images are shown (Scale bar: 1 mm). B) The F.I. values of the coated surfaces are depicted. The control group represents the F.I. of uncoated well plate surfaces. Statistically significant differences are denoted by symbols: *$p$ < 0.0001 (Unc: uncoated, Col I: Collagen I, Col IV: Collagen IV, Lam: Laminin, Fib: Fibronectin, PLL: Poly-L-lysine, Gel: Gelatin, GG: Gellan Gum, FGA: Fluoresceinyl glycine amide, FITC: Fluorescein isothiocyanate, FAM: 6-carboxyfluorescein, Rho: Rhodamine, AF488: Alexa Fluor 488, *N.D.*: Not detected).

## 1.3.4 Validation of DFATs

The dedifferentiation process in mature adipocytes involves actin remodeling upon adherence to a surface, leading to dynamic cellular deformation and secretion of lipid droplets. As a result of these morphological changes, the lipid-secreting cells acquire a fibroblastic appearance. In this context, the actin myofibrils of DFAT cells were visualized using F-actin immunostaining. Furthermore, during the transformation of mature adipocytes into DFAT cells, they express stem cell markers such as Oct-4, Sox2, c-Myc, and Nanog, acquiring mesenchymal stem cell (MSC)-like properties. Cytoplasmic expression of Oct-4 in DFATs confirms their stemness (**Figure 1-5A**).

To validate the multilineage differentiation capability of DFATs, the cells were induced to differentiate into three distinct lineages: osteogenic, chondrogenic, and adipogenic. After 21 days of osteogenic differentiation, calcium deposits in osteoblasts were assessed using Alizarin Red S staining. For chondrogenic differentiation, the production of proteoglycan compounds was detected with Alcian Blue staining on day 14. Adipogenic differentiation was confirmed by visualizing and staining lipid droplets with Oil Red O on day 14 (**Figure 1-5B**). Furthermore, in accordance with the guidelines of the International Federation of Adipose Therapeutics and International Society for Cellular Therapy, MSCs must exhibit certain surface antigens: CD44, CD73, CD90, and CD105. According to flow cytometry analyses conducted in triplicate, DFATs obtained in this study were positive for CD44, CD73, CD90, and CD105 (**Figure 1-5C**). Taken together, these results provide evidence that the obtained DFATs exhibit multipotent stem cell characteristics.

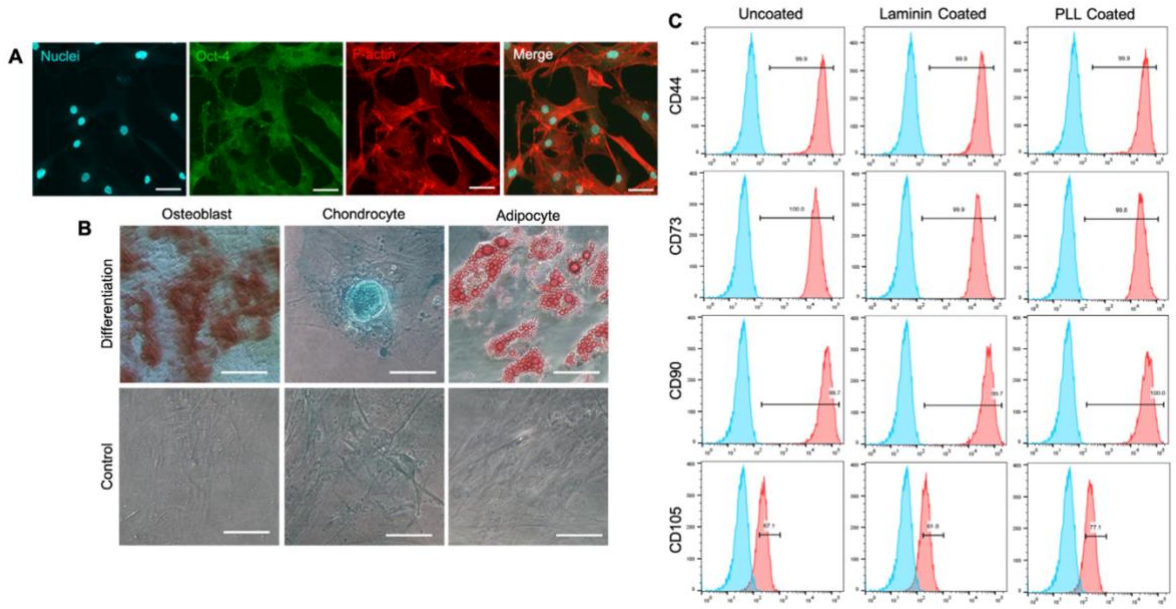


**Figure 1-5.** A) Immunofluorescence staining of Oct-4 (green), actin myofibrils (red) of DFATs, and Hoechst counterstaining was used to visualize nuclei (blue) of DFATs. The colocalization of Oct-4, F-actin and nuclei of DFATs are shown in Merge image (Scale bars: 50 µm). B) Multilineage differentiation of DFATs. Osteogenic differentiation indicated by alizarin red S staining on day 21 (left), Chondrogenic differentiation indicated by Alcian blue staining on day 14 (middle), Adipogenic differentiation indicated by oil red o staining on day 14 (right) (Scale bar: 100 µm). C) Representative flow cytometry histograms of dedifferentiated fat cells (DFATs) obtained from uncoated, Laminin coated and PLL coated surfaces at passage 4 (n=3).

## 1.4 Conclusion

In our study, we aimed to manipulate the adhesion and dedifferentiation process of mature white adipocytes on surfaces by employing physicochemical surface modifications using proteins and charged polymer coatings. Our findings demonstrated that the ratio of DFAT cells can be enhanced on surfaces coated with ECM and BM proteins, as well as cationic polymers, whereas anionic polymer coatings had the opposite effect. There are several potential reasons for the increased cell attachment and DFAT formation observed. Firstly, ECM and BM proteins likely promoted dedifferentiation by enhancing the adsorption of mature adipocytes thus increased cellular adhesion can facilitate the dedifferentiation (**Figure 1-6A**). On one hand, coating with cationic polymers might have enhanced the adsorption of serum proteins onto the surface, thereby increasing the adhesion of mature adipocytes and consequently improved the DFAT ratio (**Figure 1-6B**). This process could involve electrostatic interactions between the negatively charged cell membrane and the positively charged polymer coating, along with integrin-mediated biological mechanisms. Conversely, coating with anionic polymers could have reduced the DFAT ratio by diminishing both the adhesion of the negatively charged cell membrane to the surface and the adsorption of serum proteins, following a similar logic of electrostatic interactions (**Figure 1-6C**).

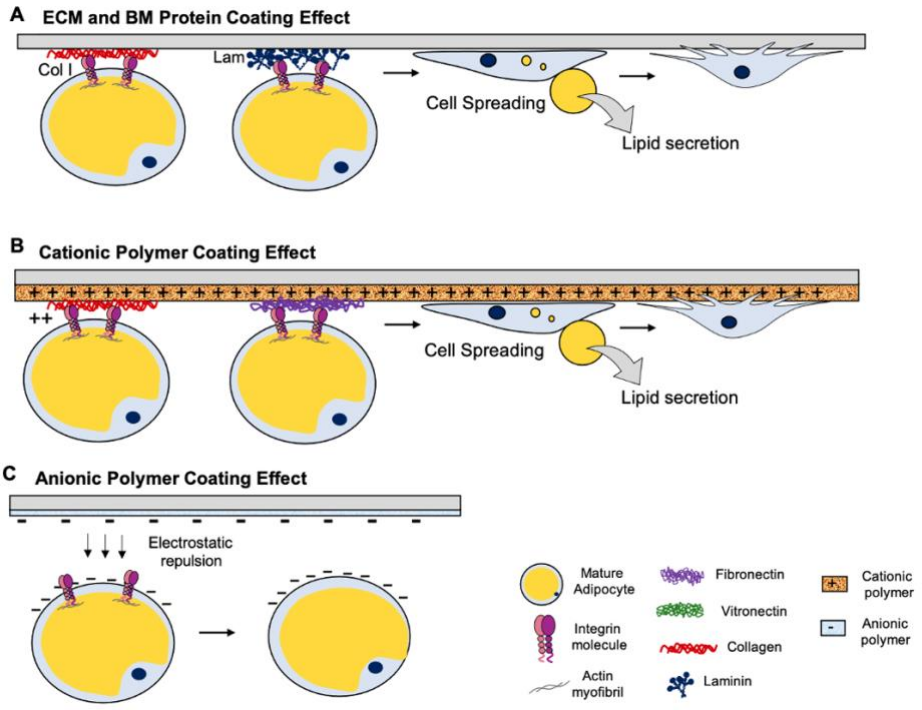


*(Figure caption is on next page.)*

**Figure 1-6.** A) Adsorbed ECM and BM proteins might increase mature adipocyte attachment, thus increase DFAT ratio. B) Electrostatic interaction between cell and coated surface might increase protein adhesion, thus cell attachment and DFAT ratio. C) Electrostatic repulsion between cell and surface might decrease the cell attachment and then dedifferentiation of mature adipocytes.

## 1.5 Reference


1. F. Louis and M. Matsusaki, *Biomater. Organ Tissue Regener*. Woodhead Publishing, **2020**. 393.
2. S. Miettinen, J. R. Sarkanen, N. Ashammakhi, *Topic Tis. Eng.* **2008**, *4*, 26.
3. E. D. Rosen, O. A. MacDougald, *Nat. Rev. Mol. Cell Biol*. **2006**, *7*, 885.
4. B. D. Pope, C. R. Warren, K. K. Parker, C. A. Cowan, *Trends Cell Biol*. **2016**, *26*, 745.
5. A. Sakers, M. K. de Siqueira, P. Seale, C. J. Villanueva, *Cell* **2022**, *185*, 419.
6. X. Peng, T. Song, X. Hu, *Biomed. Res. Int*. **2015**, *2015*, 673651.
7. T. Matsumoto, K. Kano, D. Kondo, *J. Cell Physiol*. **2008**, *215*, 210.
8. M. Jumabay, *World J. Stem Cells* **2015**, *7*, 1202.
9. H. Fujimaki, H. Matsumine, H. Osaki, *Regen. Ther*. **2019**, *11*, 240.
10. T. Kazama, M. Fujie, T. Endo, K. Kano, *Biochem. Biophys. Res. Commun*. **2008**, *377*, 780.
11. M. Shimizu, T. Matsumoto, S. Kikuta, et al. *J. Orthop. Sci.* **2018**, *23*, 688.
12. T. Yanagi, H. Kajiya, S. Fujisaki, *Regen. Ther*. **2021**, *18,* 472.
13. X. Hu, P. Luo, X. Peng, *Gen. Comp. Endocrinol*. **2015**, *214*, 77.
14. H. Sugihara, N. Yonemitsu, S. Miyabara, K. Yun, *Differentiation* **1986**, *31*, 42.
15. J. A. Côté , J. Lessard, M. Pelletier, *FEBS Open Bio*. **2017**, *7*, 1092.
16. J. Lessard, J. A. Côté, M. Lapointe, *JOVE,* **2015**, *2015*, 52485.
17. L. Liu, X. Liu, M. Liu, Y. Jihu, D. Xie, H. Yan, *Exp. Cell Res*. **2022**, *415*, 113109.
18. J. Kim, K. Y. Park, S. Choi, *Lab Chip*. 2022, 22, 3920.
19. E. G. Hayman, M. D. Pierschbacher, S. Suzuki, E. Ruoslahti, *Exp. Cell Res*. **1985**, *160*, 245.
20. J. G. Steele, C. L. McFarland, B. Ann Dalton, *J Biomat. Sci. Pol. Ed*. **1994**, *5*, 245.
21. M. Ferrari, F. Cirisano, M. Carmen Morán, *Colloids Interfaces* **2019**, *3*, 48.
22. E. M. Harnett, J. Alderman, T. Wood, *Colloids Surf. Biointerfaces* **2007**, *55*, 90.
23. G. Altankov, K. Richau, T. Groth, *Materialwiss. Werkstofftech*, **2003**, *34*, 1120.
24. O. V. Bondar, D. V. Saifullina, I. Shakhmaeva, I. Mavlyutova, T. I. Abdullin, *Acta Naturae* **2012**, *4*, 78.
25. D. Fischer, Y. Li, B. Ahlemeyer, J. Krieglstein, T. Kissel, *Biomaterials* **2003**, *24*, 1121.

# Chapter 2

## Cationic Polymer Effect on Brown Adipogenic Induction of Dedifferentiated Fat Cells

## 2.1 Introduction

Obesity, characterized by excessive body fat, is a global health issue[1] and a significant risk factor for diseases like type 2 diabetes,[2] high blood pressure,[3] heart disease,[4] stroke,[5] certain cancers,[6] musculoskeletal problems,[7] and respiratory issues.[8] The 2023 World Obesity Atlas predicts that by 2035, nearly two billion people worldwide will be affected by obesity.[9]

The rise in obesity underscores the importance of understanding adipose tissue and its metabolic complexities. Adipose tissue in mammals is mainly of two types: WAT, which stores energy and secretes hormones, and BAT, which regulates body temperature through non-shivering thermogenesis.[10] BAT's abundant mitochondria and the protein UCP1 enable it to convert energy into heat, impacting calorie expenditure and making it a potential target for obesity treatments.

White adipocytes are highly plastic and can reprogram into DFAT cells, a type of stem cell with multipotent characteristics similar to mesenchymal stem cells (MSC).[11] These DFAT cells can differentiate into various lineages, making them valuable for tissue engineering, regenerative medicine, cell therapy, and stem cell research. DFAT cells are easily and abundantly obtained from waste adipose tissue through procedures like liposuction, providing an advantage over other stem cell sources.

Engineering adipose tissue is promising for enhancing endocrine metabolism.[12–14] Various scaffold materials, including collagen type I,[15] hyaluronic acid,[16] gelatin,[17] and polyethylene glycol (PEG) derivatives,[18] have been explored to support adipose tissue functions. However, there has been limited research on using thermogenic adipose tissue engineering to treat obesity-related diseases.

In this chapter, we used fibrin gel, known for its biocompatibility and biodegradability, as the base material for constructing adipose tissues. Although fibrin gels alone have limited

impact on adipogenesis,[19] they provide a suitable environment for soft tissue engineering. When combined with collagen microfibers (CMF), fibrin gels support high cell viability and structure regeneration of adipose tissue.[20] However, no studies have examined the effect of fibrin mixed with various polymers on brown adipogenic redifferentiation of DFATs.

In this chapter, we aimed to create brown-like adipose tissue by encapsulating DFATs from human white adipocytes in fibrin gel mixed with biopolymers such as Col I, Col IV, Fib, Lam, Gel, GG and PLL. We assessed the impact of these polymers on browning through lipid droplet size analysis, mitochondrial assessment, oxygen consumption rates, and real time quantitative polymerase chain reaction (RT-qPCR) analysis. This research could significantly advance thermogenic adipose tissue engineering and offer new approaches to tackling obesity and related health issues.

## 2.1 Experiments

### 2.1.1 Materials

Fibrinogen (from bovine plasma, F8630), Thrombin (from bovine plasma, T4648), Fibronectin (from human plasma, F2006), Collagen type IV (from human placenta, C7521), Poly-L-lysine (PLL, P4707), Poly-L-lysine FITC conjugated (P3543), Phosphate buffered saline powder (PBS, D5652), Collagenase from *Clostridium histolyticum* (Type I, C0130) and Triton-X 100 (T8787), Bovine Serum Albumin (BSA, 3294), Dexamethasone (D4902), Indomethacin (I7378) 3-Isobutyl-1-methylxanthine (IBMX, I5879), Insulin (I6634) Rosiglitazone (R2408), 3,3′,5-Triiodo-L-thyronine sodium salt (T3, T6397), Hoechst 33324 (H3570) were purchased from Sigma-Aldrich (St Louis, MO, USA). Trypan Blue (T10282), MitoTracker™ Deep Red FM (M7212), UCP1 polyclonal antibody (PA1-24894), Qubit HS DNA Assay Kit (Q3285), Anti-rabbit secondary antibody Alexa Fluor® 647, Nile Red (N1142), PicoPure™ RNA Isolation kit (KIT0204) Penicillin, Streptomycin were obtained from Thermo Fisher Scientific (Whaltam, MA, USA). Gelatin (077-03155), 4%-paraformaldehyde (16310245), $Na_2SO_3$ (198-03412), Trypsin (207192-83) were purchased from Wako Pure Chemical Industries (Tokyo, Japan). Collagen type I FAM conjugated (AS-85111) obtained from Funakoshi (Tokyo, Japan). Anti Heperan Sulphate (370255-S) was purchased from AMS Biotechnology (Abingdon, UK). Dulbecco's Modified Eagle Medium (DMEM) high glucose (08458-16) was came from Nacalai Tesque Inc. (Kyoto, Japan). Anti-mouse Heparan Sulphate antibody (370255-S) purchased from AMS Biotechnology (Europe)

Limited, Abingdon, UK. Human UCP1 ELISA Kit (MBS451508) was purchased from MyBioSource (San Diego, USA). Oxoplate 96-well round-bottomed OxoPlate (OP96U) was came from PreSens Precision Sensing, (Regensburg, Germany). Live/Dead® viability assay kit (PK-CA707-30002) purchased from PromoKine (Heidelberg, Germany). Phosphate Buffer Saline (PBS, 14249-24) was came from Nacalai Tesque Inc. (Kyoto, Japan). Fetal Bovine Serum (FBS, 10270106) was obtained from Gibco. Adipocyte Differentiation medium (811D-250) was came from Cell Applications Inc. (San Diego, USA). Collagen type I (from bovine dermis, Atelocell, IPC-50) was purchased from Koken (Tokyo, Japan). Laminin (354259) was obtained from Corning (Arizona, USA). Gellan Gum (8H1121A) was came from Sansho (Osaka, Japan). Phalloidin-iFluor 594 Reagent (ab176757 purchased from Abcam (Cambridge, UK). RNase-free DNase set (79254) was purchased from Qiagen (Hilden, Germany). iScript™ cDNA Synhtesis Kit, Bio-Rad (California, USA). TaqMan gene expression assays (Applied Biosystems) was purchased from Thermo Fisher Scientific (Whaltam, MA, USA).

### 2.1.2 BAT drop seeding

The sample preparation is shown in **Figure 2-1**. DFATs were mixed at a seeding density of $4.0 \times 10^6$ cells/mL with a fibrinogen solution (6 mg/mL) and a thrombin solution (3 U/mL), both filtered using a 0.2 μm filter. The mixture was seeded into a 96-well plate at 5 μL and incubated at 37°C for 20 minutes for gelation. After adding 80 μL of growth medium (GM, 10 % FBS and 1% Antibiotics in DMEM high glucose), samples were transferred to a 24-well plate and incubated in 500 μL of GM for 2 days. The medium was then replaced with brown adipogenic differentiation medium (BAM) containing various components including T3 and insulin, following the reported browning protocol.[18] For polymer-mixed drops, polymers were dissolved in PBS, filtered, and mixed with the cell-fibrin gel mixture at 50 μg/mL, except for PLL which was used at 5, 10, or 20 μg/mL. Samples were cultured in BAM for 2 weeks, with the medium replaced every two days. To obtain WAT drops, samples were cultured in Human Adipocyte Differentiation Medium (Cell Application, Inc.) for 2 weeks, with medium changes every two days. For undifferentiated DFAT drops, samples were cultured in GM for the same duration with medium changes every two days.

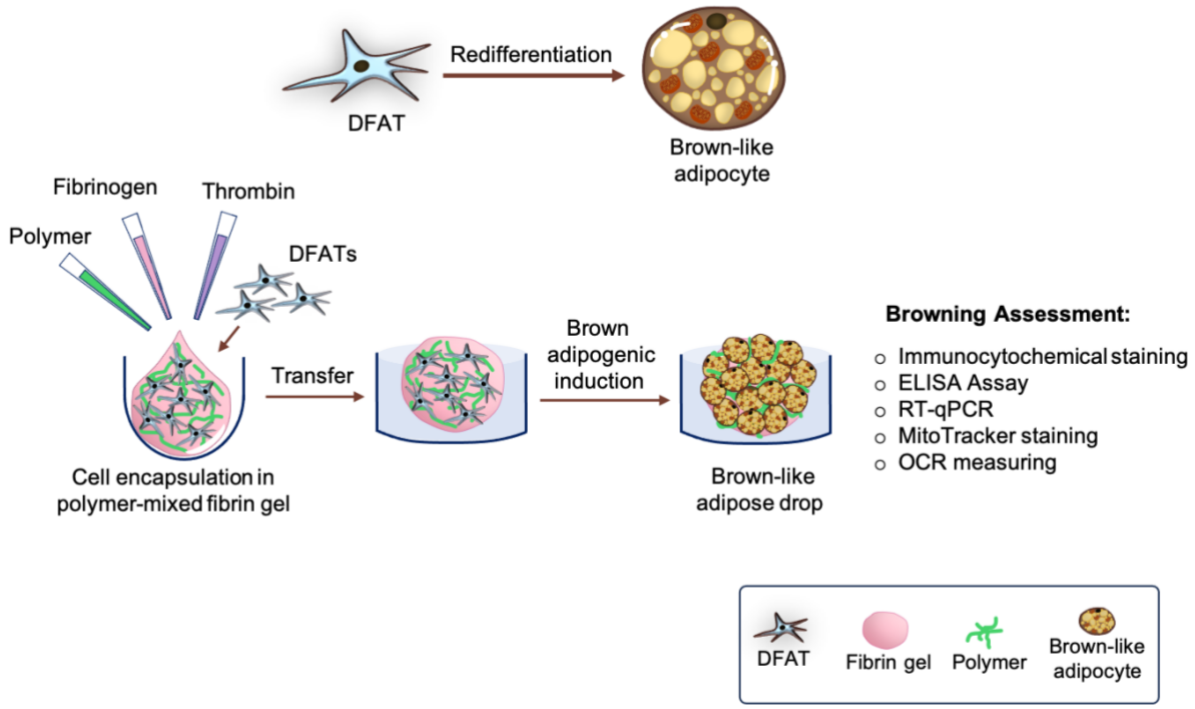


**Figure 2-1.** Schematic overview of the research design. DFATs were encapsulated within a fibrin gel by using a round bottom 96 well plate with variety of polymers, then samples transferred into an ultra-low attachment 24 well plate and cultured in brown adipogenic medium for 2 weeks. Mixed polymers are collagen I, collagen IV, fibronectin, laminin, gelatin, and gellan gum, and PLL.

### 2.1.3 Immunofluorescence imaging

After 2 weeks of incubation in BAM and WAM, samples were washed with PBS, then fixed in 4% paraformaldehyde in PBS overnight at 4°C. Then, they were treated with 0.05% Triton X-100 for 15 minutes for permeability, followed by 1% BSA in PBS for 1 hour to reduce nonspecific staining. They were incubated with anti-UCP1 antibody (1:500 dilution) overnight at 4°C, then with Alexa Fluor 647 secondary antibodies (1:200) for 2 hours at room temperature. Lipid accumulation was visualized with Nile Red (50 ng/mL), and nuclei were counterstained with Hoechst (10 ng/mL).

For mitochondrial staining on days 7 and 14, samples were incubated with MitoTracker dye in medium for 30 minutes at 37°C in a 5% $CO_2$ incubator. All samples were washed with PBS and examined using an FV3000 Confocal Laser Scanning Microscope (CLSM) (Olympus, Tokyo, Japan). Z-stack images were captured, and maximum intensity projection was performed, maintaining consistent exposure time and excitation power for all samples. Data

were acquired by measuring the total fluorescence intensity of UCP1, lipid droplets, and MitoTracker, normalized to Hoechst F.I. using Image J software.

For heparan sulfate staining, DFATs were incubated with FITC-labeled PLL (10 µg/mL) in GM on a 96-well plate. After 24 hours at 37°C in a 5% $CO_2$ incubator, cells were fixed, permeabilized, and blocked. Anti-heparan sulfate antibody (1:100) was applied overnight at 4°C, followed by Alexa Fluor® 647 secondary antibodies (1:200) for 2 hours at room temperature. Nuclei were counterstained with Hoechst, and all samples were examined using the FV3000 CLSM (Olympus, Tokyo, Japan).

### 2.1.4 Lipid size measurement

Samples incubated in BAM and WAM were stained for intracellular lipid accumulation with Nile Red, and nuclei were counterstained with Hoechst. Then, they were rinsed in PBS and examined using an FV3000 CLSM (Olympus, Tokyo, Japan) at 60x magnification with immersion oil. Lipid droplet sizes were quantified using Image J, with 200 droplets measured per image.

### 2.1.5 Cell viability assay

To assess cell viability in PLL-mixed drops with varying PLL concentrations (0, 10, and 50 µg/mL), samples were cultured in GM overnight. A Live/Dead cell viability assay kit was then applied and compared to samples containing only fibrin. After three PBS washes, cells were stained with Calcein (2 µM for live cells) and Ethidium Homodimer-1 (4 µM for dead cells) for 30 minutes at 37°C in the dark. Imaging was performed using an FV3000 CLSM (Olympus, Tokyo, Japan). Cell viability percentages were quantified using Image J software on Z-stack images, captured with consistent laser power and step sizes.

### 2.1.6 Gene expression assay

Gene expressions were assessed using RT-qPCR. Total RNA from drops (6 drops per replicate) was isolated using a PicoPure™ RNA isolation kit. The RNA was quantified with a Nanodrop™ N1000 device. RNA was converted to DNA using an iScript cDNA synthesis kit. cDNA was amplified with TaqMan Fast Advanced Mix and TaqMan gene expression assays for UCP1, Cidea, PRDM16, and RPII (housekeeping gene) shown as **Table 2-1**. The cDNA

synthesis and RT-qPCR were performed using a StepOnePlus Real-Time PCR System. RT-qPCR analysis was conducted on cells from three different donors, with 3 to 9 replicates in total.

**Table 2-1.** TaqMan probes used for RT-qPCR experiments

| Gene Symbol | Assay ID |
|---|---|
| RPII | Hs00172187_m1 |
| UCP1 | Hs01084772_m1 |
| PRDM16 | Hs00223161_m1 |
| Cidea | Hs00154455_m1 |

### 2.1.7 Measurement of oxygen consumption rate

Polymer-mixed samples were washed with PBS and transferred to a 96-well OxoPlate (OP96U, PreSens). Four drops per well were added with DMEM (10% FBS, 1% penicillin-streptomycin, no phenol red). For calibration, eight wells were used for 0% $O_2$ ($H_2O$ with 10 mg/mL sodium sulfite) and 100% $O_2$ (respiration media). Oxygen concentrations were measured on day 14 and after 24 hours using a plate reader with two calibration standards and filters for the indicator (excitation 540 nm, emission 650 nm) and reference (excitation 540 nm, emission 590 nm). Data were normalized using DNA quantification with a Qubit HS DNA assay.

### 2.1.8 DNA quantification

A Qubit™ DNA HS Assay Kit with a Qubit™ 2.0 Fluorometer (Life Technologies, ThermoFisher Scientific Inc.) was used to quantify DNA. Samples were washed with PBS, treated with Trypsin-EDTA to dissolve the fibrin gel, and subjected to three cycles of freezing and thawing in Eppendorf tubes. The assay was conducted according to the manufacturer's instructions.

### 2.1.9 Monitoring of T3 and insulin adsorption of PLL coated surfaces

The PLL coating was applied as per the manufacturer's protocol, involving a 5-minute incubation at room temperature with the addition of 200 µL solution onto a 24-well polystyrene surface. Insulin and T3 solutions were prepared following the manufacturer's data sheet and

added to the PLL-coated wells. Samples were then collected every 10 minutes, and UV-Vis absorbances were measured using a UV-Vis/NIR Spectrophotometer (V 670, Jasco Inc., Japan) with final concentrations of 1 µM for T3 and 10 µM for insulin. The adsorbed product amount on the surface over time was calculated based on the absorbance data (n=3).

### 2.1.10 Zeta potential measurement

The zeta potential of insulin and T3 solutions was measured using a Malvern ZetaSizer. Solutions were prepared at concentrations matching those in BAM (120 nM for T3 and 850 nM for insulin). Disposable folded capillary cells were filled with 800 µL of each solution, and measurements were conducted via dynamic light scattering at 25°C (n=3).

***Statistical Analysis*:** ANOVA analyses were conducted using ezANOVA software to assess differences between data sets. Error bars denote standard deviation, and *p*-values < 0.05 were considered statistically significant.

## 2.3 Results

### 2.3.1 Brown adipogenic differentiation medium effect on browning

First, the brown adipogenic induction potential of our culture conditions was confirmed by comparing BAM and WAM in drop tissue formation. Lipid droplet sizes of differentiated brown and white adipocytes are well-defined in literature.[21] The morphology of lipid droplets in brown and white adipocytes demonstrates notable differences, with intracellular lipid droplets appearing large and uniocular in WAT and small and multilocular in BAT. Thus, we compared the effects of these media on lipid droplet sizes. After 14 days of culture, lipid droplets in samples from BAM and WAM were stained with Nile Red, as shown in **Figure 2-1A**. Significantly smaller ($p<0.001$) lipid droplet diameters were observed in brown-differentiated cells compared to white-differentiated cells. Brown adipocytes exhibited lipid droplet sizes of 2.4 (± 0.8) µm, whereas white-differentiated cells had larger droplets measuring 7 (± 3) µm (**Figure 2-1B**), confirming morphological differences between white and brown adipogenic differentiations.

BAT is known for its high mitochondrial content. Therefore, mitochondrial content in brown-differentiated cells and undifferentiated cells (BAM and GM, respectively) was

evaluated by quantifying mitochondrial abundance through MitoTracker staining, as illustrated in **Figure 2-1C**. The results showed significantly higher fluorescence intensity of mitochondria in brown-differentiated cells compared to undifferentiated cells, with a 25% increase (±17, $p<0.05$) shown in **Figure 2-1D**. The successful occurrence of brown adipogenic differentiation was confirmed by the increased mitochondrial content in the brown-differentiated cells.

Immunocytochemical visualization of the brown adipogenic marker UCP1 and lipid droplets was then performed on both brown adipogenic differentiated and undifferentiated samples cultured in BAM, GM, and WAM, as shown in **Figure 2-1E**. Distinct expressions of UCP1 and lipid droplet accumulations were exclusively observed in the BAM group, confirming successful brown adipogenic differentiation. As expected, WAM cultured droplets showed lipid accumulation but were negative for UCP1 expression. **Figure 2-1F** shows a higher magnification view of samples cultured in BAM.

Finally, relative gene expression levels of BAT-specific genes (UCP1, Cidea, PRDM16) were assessed by RT-qPCR analysis. UCP1 serves as a primary thermogenic marker crucial for fatty acid metabolism.[22] The results demonstrated markedly elevated expressions of these brown adipogenic-related genes in BAM groups compared to GM counterparts (**Figure 2-1G**). Specifically, UCP1, Cidea, and PRDM16 gene expressions were 58 (± 16), 198 (± 71), and 4.7 (± 0.8) times higher, respectively, in BAM groups, highlighting significant differences in brown-specific gene expression indicative of browning.

Based on comprehensive evaluations across various parameters, BAM exerted a notable impact on DFATs encapsulated in fibrin gel and cultured for 14 days in terms of promoting browning. This efficacy was evident in measurements of lipid droplet size, mitochondrial abundance, immunocytochemical UCP1 expression, and gene expression of BAT markers. Consequently, BAM and fibrin gel culture conditions were selected for subsequent investigations into the effects of various added polymers.

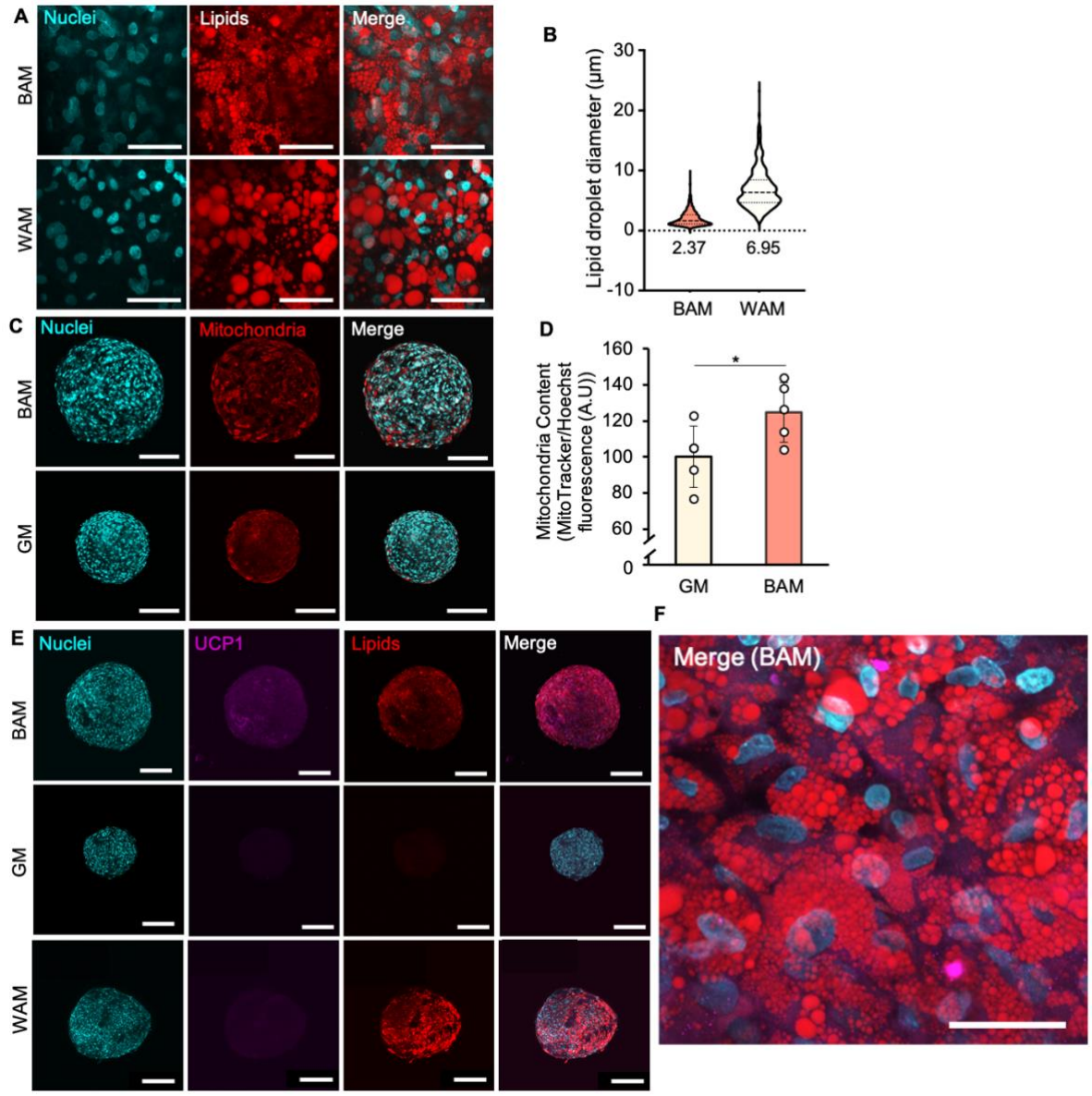


**Figure 2-1.** A) Lipid droplets in differentiated cells were stained with Nile Red, and nuclei were visualized using Hoechst counterstaining (scale bar: 50 µm).B) Lipid droplet sizes were quantified using Image J, measuring 200 lipid vesicle diameters per drop (n=3, from one donor). C) Representative MitoTracker staining images of mitochondria (red) and Hoechst counterstaining for nuclei (blue) in drops incubated in BAM and GM on day 14. Merge image shows mitochondria and nuclei (scale bar: 200 µm).D) MitoTracker fluorescence measurements in drops incubated in BAM and GM, normalized to DNA (Hoechst) fluorescence. Results are mean ± standard deviation (n=5, from one donor), * = $p < 0.05$. E) Representative images of immunocytochemical staining for Uncoupling Protein 1 (UCP1, magenta), lipid droplets (red, Nile Red), and nuclei (blue, Hoechst) in drops incubated in BAM, GM, and white adipogenic differentiation medium (WAM) on day 14. Merge image shows UCP1, lipids, and nuclei (scale bar: 200 µm). F) Higher magnification of UCP1, lipids, and nuclei in drops cultured in BAM (scale bar: 50 µm). G) Relative gene expressions of brown adipogenic markers on day 14: Uncoupling Protein 1 (UCP1), Cell Death-Inducing DNA Fragmentation Factor Alpha-Like Effector A (Cidea), and PR Domain Containing 16 (PRDM16). Results are mean ± standard

deviation (n=3, from one donor), normalized to RNA Polymerase II (RPII, housekeeping gene). Statistical differences were determined by Student's *t*-test, * = $p < 0.05$, ** = $p < 0.01$. White dots represent data points from each parallel experiment.

### 2.3.2 Determining the optimum PLL concentration for BAT drops

PLL's cytotoxic potential[23] prompted evaluation before its inclusion in fibrin gel tissues, with varied concentrations tested. Other polymers were added at 50 µg/mL as per our previous protocol. Based on cell viability data obtained by Live/Dead staining (**Figure 2-2A**), PLL at 50 µg/mL resulted in 26% viability, while lower concentrations exceeded 80% (**Figure 2-2B**). Consequently, PLL concentration was maintained at 10 µg/mL for subsequent browning experiments. In addition, to evaluate concentration effect on browning PLL 5 and 20 µg/mL PLL concentrations samples were also prepared for gene expression analysis.

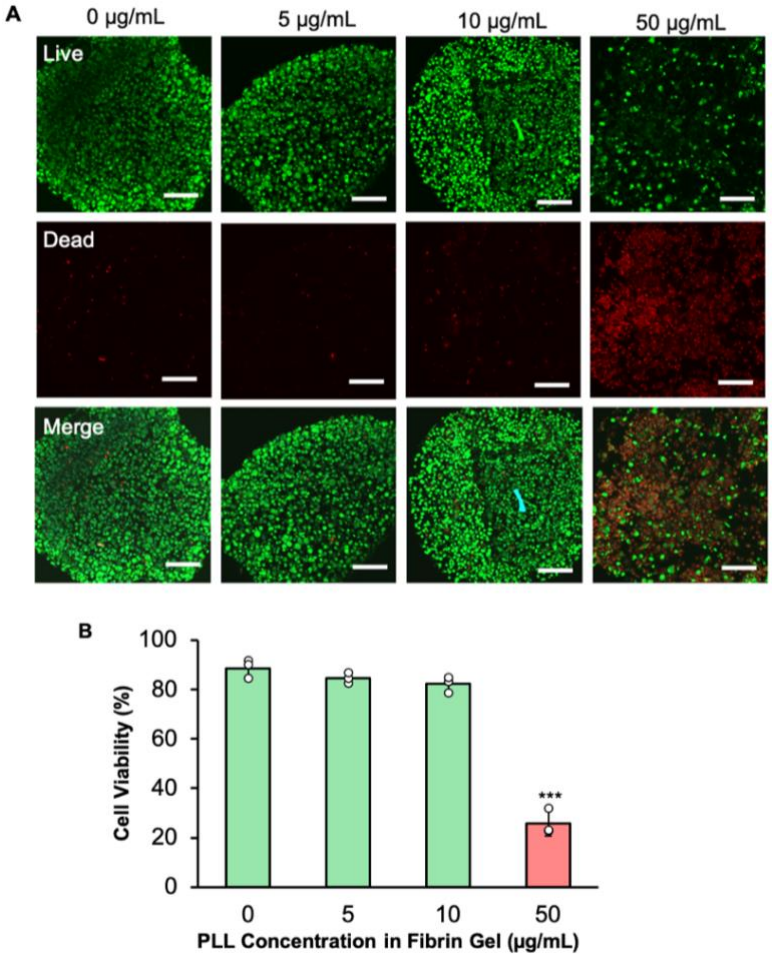


**Figure 2-2.** A) Representative Live/Dead staining of PLL-mixed fibrin gel drops at 0 (fibrin only), 5, 10, and 50 µg/mL concentrations (Scale bar: 200 µm). B) Quantification of cell viability using Image J. Results are presented as means ± s.d. of experiments conducted on n=3 independent samples from one donor. Statistical differences were determined using ANOVA tests and indicated as *** = $p < 0.001$. White dots represent individual data points.

### 2.3.3 UCP1 and lipid contents of polymer-mixed samples

UCP1 immunofluorescence staining (**Figure 2-3A**) confirmed brown adipogenic differentiation of DFATs in fibrin-only and polymer-mixed fibrin gel by day 14 in BAM conditions. Quantification of UCP1 and lipid content (**Figure 2-3B**, white bars) normalized by DNA fluorescence showed PLL as the sole polymer UCP1 intensity by 1.5 times (± 0.2) compared to fibrin-only, though not statistically significant ($p > 0.0509$). No significant differences were observed in lipid content among polymer-mixed groups versus fibrin-only (**Figure 2-3B**, red bars), except between specific pairs like PLL vs. GG and fibronectin. PLL notably exhibited the highest lipid content (1.1 ± 0.1). Immunofluorescent images suggest PLL might enhance both UCP1 expression and lipid content. ELISA result (**Figure 2-3C**), normalized by DNA, confirmed PLL's highest relative UCP1 concentration (5 ± 2) compared to fibrin-only, with similar trends in gelatin, laminin, and fibronectin mixes, albeit to a lesser extent, supporting PLL's role in inducing brown adipogenesis.

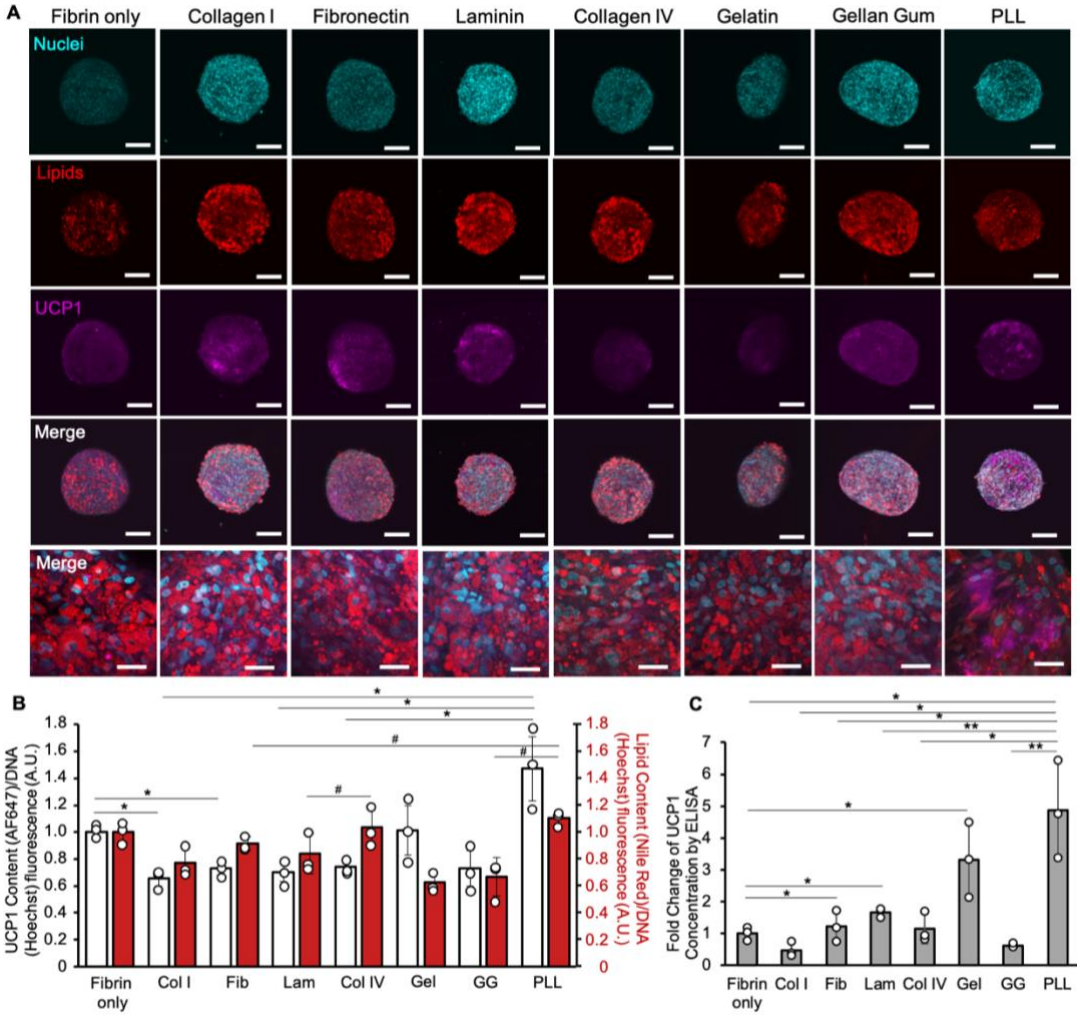


*(Figure caption is on next page.)*

**Figure 2-3.** A) Representative images of UCP1 (magenta), Nile Red-stained lipid droplets (red), and Hoechst-stained nuclei (blue) in polymer-mixed brown-like adipose drops on day 14. Merge images show UCP1, lipids, and nuclei (Scale bar: 200 µm; for high magnification Merge image scale bar: 50 µm). B) Quantification of UCP1 (light grey bars) and Nile Red fluorescence (red bars) in drops, normalized by DNA (Hoechst) fluorescence. Results are presented as mean ± standard deviation (n=3, three independent samples from one donor). Statistical differences were determined using ANOVA tests and indicated as * = $p< 0.05$ for UCP1, # = $p< 0.05$ for lipids. C) ELISA results for UCP1 in polymer-mixed drops. Results are shown as mean ± standard error (n=3, three independent experiments from one donor). Statistical differences were determined using ANOVA tests and indicated as * = $p< 0.05$. White dots represent data points for each sample.

## 2.3.4 Relative gene expression analysis of polymer-mixed BAT drops

The gene expression of brown adipogenic markers UCP1, Cidea, and PRDM16 was analyzed to confirm DFATs' redifferentiation in fibrin-only and polymer-mixed fibrin gels (**Figure 2-4**). PLL-mixed drops (10 µg/mL) significantly increased UCP1 gene expression by 6-fold (± 3) compared to fibrin only. Increasing PLL concentrations (5, 10, and 20 µg/mL) in polymer-mixed droplets also showed corresponding increases in UCP1 expression (1 ± 0.3 to 2.07 ± 0.01) (**Figure 2-4A**, right graph), affirming PLL's significant role in inducing brown adipogenesis. For Cidea gene expression (**Figure 2-4B**), PLL (10 µg/mL) exhibited the highest expression at 3 (± 3), with minimal impact from PLL concentration variations (up to 1.1 ± 0.3 for 20 µg/mL). PRDM16 relative gene expression did not show significant differences, but PLL (10 µg/mL) demonstrated a similar increasing trend as observed for UCP1 and Cidea. Overall, PLL promoted the expression of brown-specific genes, particularly UCP1, indicating its crucial role in brown adipogenesis induction. However, increased PLL concentrations did not consistently lead to significant differences, except for UCP1 gene expression ($p < 0.01$). One possible reason for the high error bars in **Figure 2-4** could be the age-related decrease in the cellular differentiation abilities of DFATs from different donors. Increased donor age has been reported to negatively impact stem cell differentiation in various studies. Therefore, cells from donors aged 41 to 53 may contribute to the high standard deviations. Additionally, while increased PLL concentration significantly boosts UCP1 gene expression (**Figure 2-4A**, right chart), there is no significant difference in Cidea and PRDM16 gene expressions between the groups. This could be because Cidea and PRDM16 are early gene markers compared to UCP1, whose expression decreases as UCP1 expression increases. Considering the cytotoxicity associated with higher polycation concentrations, we concluded that a moderate concentration is more advantageous for this study.

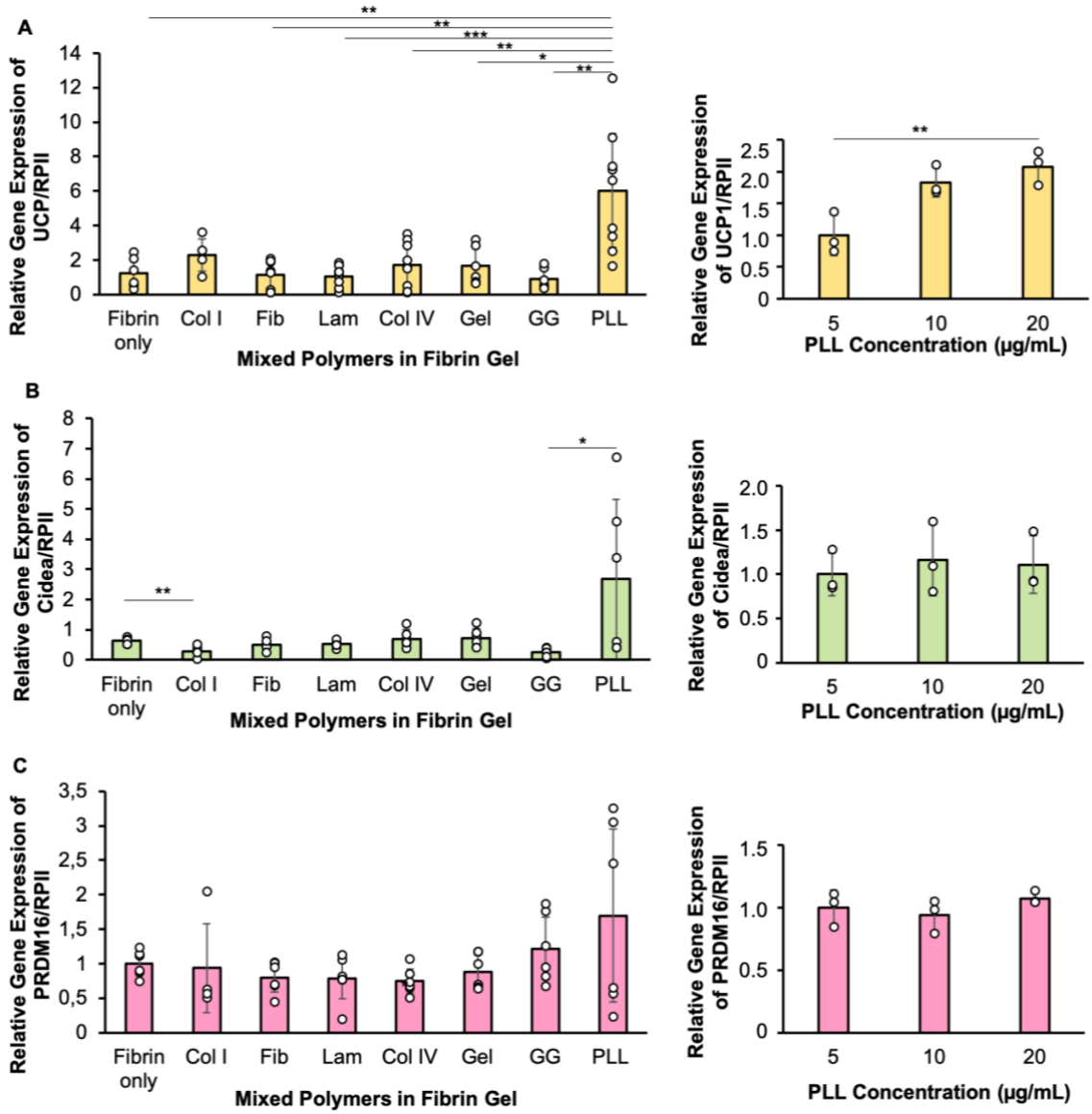


**Figure 2-4.** Relative gene expressions of several brown adipogenic markers. A) Uncoupling protein 1 (UCP1), results are shown as mean ± standard error. The results shown as means ± s.d. of experiments performed on N=4-9, using 3 different patients' cells for left graph, n=3 using 1 patient's cells for right graph. * = $p < 0.05$, ** = $p < 0.01$, *** = $p < 0.001$. B) Cell death-inducing DNA fragmentation factor alpha-like effector A (Cidea), the results shown as means ± s.d. of experiments performed on N=4-6, using 2 different patients' cells for left graph, n=3 using 1 patient's cells for right graph. * = $p < 0.05$, ** = $p < 0.01$. C) PR domain containing 16 (PRDM16). The results shown as means ± s.d. of experiments performed on N=4-6, using 2 different patients' cells for left graph, n=3 using 1 patient's cells for right graph. * = $p < 0.05$. PLL was used 10 µg/mL for left graph. Statistical differencies were obtained by student-t tests were shown as * = $p < 0.05$. White dots represent data points of each parallel.

### 2.3.5 Mitochondrial assessment on polymer mixed BAT drops

To assess the impact of added polymers on mitochondrial content during brown adipogenic differentiation, mitochondrial abundance in polymer-mixed samples cultured with BAM was evaluated on days 7 and 14 (**Figure 2-5A**), normalized by DNA fluorescence intensity (**Figure 2-5B**). Comparisons were made between fibrin-only samples (day 7) and polymer-mixed samples at both time points (7th and 14th days), as well as fibrin-only samples (day 14). Initially, mitochondrial abundance in polymer-containing drops on the 7th day did not surpass fibrin-only levels. PLL-containing drops showed significantly lower mitochondrial content initially but exhibited a notable increase by the 14th day, reaching 163 (± 11) compared to fibrin-only samples on day 7 (100 ± 7). Overall, mitochondrial quantity increased significantly over time across all groups, notably in laminin, collagen type IV, and GG drops compared to fibrin-only drops, suggesting ongoing brown adipogenic differentiation. Oxygen consumption rate was assessed on the 14th day, with PLL-containing drops showing the highest rate over a 24-hour period, significantly reaching 138 (± 13) compared to fibrin-only drops (100 ± 13) (**Figure 2-5C**). Conversely, collagen type I and laminin drops exhibited decreased oxygen consumption, while other groups showed values similar to fibrin-only samples. These findings underscore PLL's role in enhancing brown adipogenesis and metabolic activity.

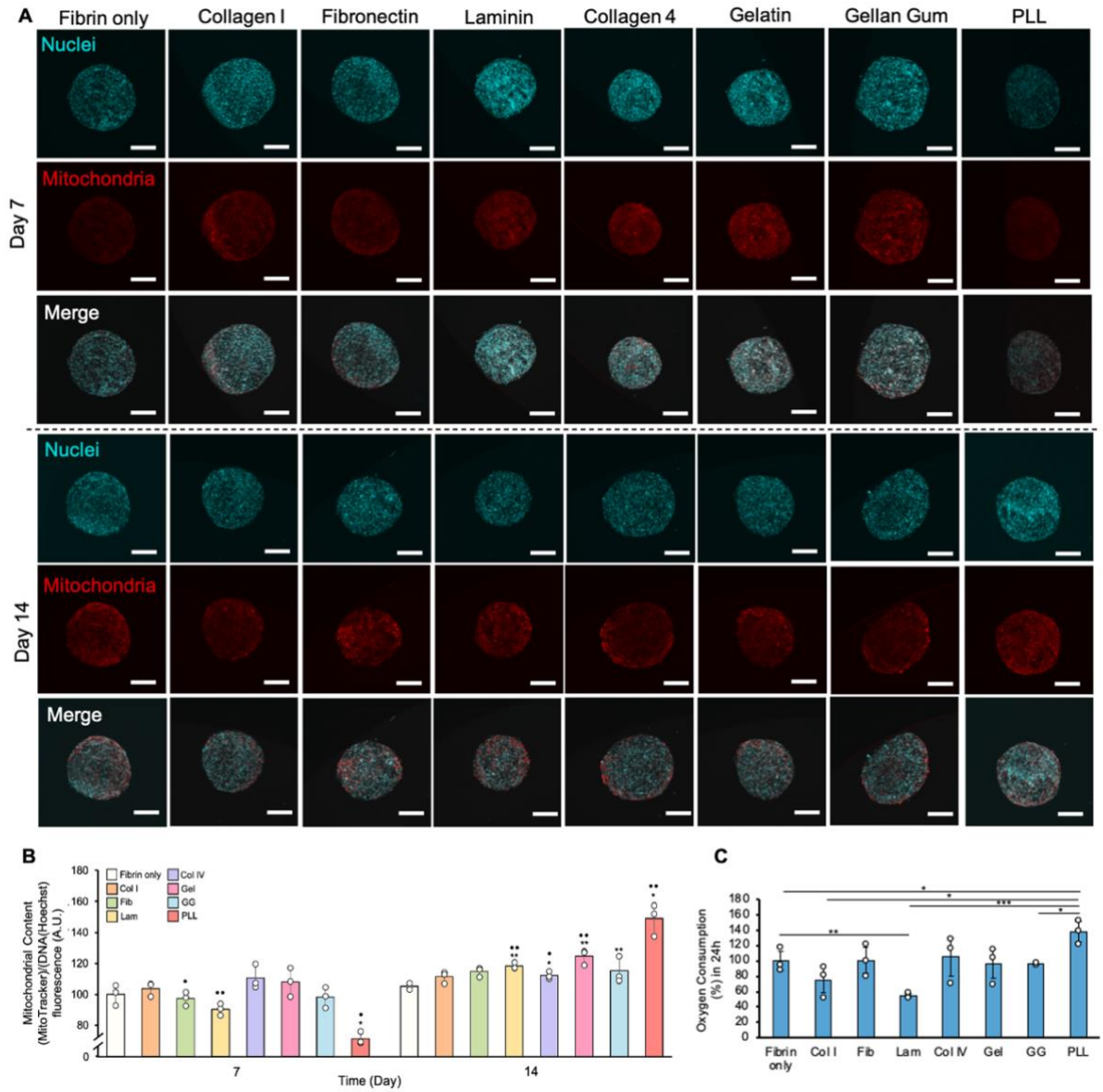


**Figure 2-5.** Representative MitoTracker staining images show mitochondria (red) and nuclei (blue) in drops incubated with BAM on days 7 and 14. The merge image displays mitochondria and nuclei (Scale bar: 200 µm). B) MitoTracker fluorescence measurements, normalized to DNA fluorescence, are shown as mean ± standard error (n=3, from one donor). Statistical differences were determined by ANOVA: * = $p < 0.05$, ** = $p < 0.01$ compared to day 7 fibrin-only group; • = $p < 0.05$, •• = $p < 0.01$ compared to day 14 fibrin-only group. C) Oxygen consumption percentages over 24 hours, shown as mean ± standard error (n=3, from one donor). Statistical differences by ANOVA: * = $p < 0.05$, ** = $p < 0.01$, *** = $p < 0.001$. White dots represent data points.

### 2.3.6 Monitoring T3 and insulin adsorption on PLL coated surfaces

Positively charged PLL can interact with negatively charged proteins, including culture medium components, potentially promoting the adsorption of hormones or proteins that induce brown adipocyte differentiation. To test this, T3 and insulin from the BAM were examined. By using their UV absorbance spectra (**Figure 2-6**), time-dependent adsorption curves of T3 and insulin on PLL-coated surfaces were observed (**Figure 2-7A** and **B**). T3 peaked at 240-300 nm and significantly accumulated after about 30 min ($p < 0.05$), while insulin peaked at 240-285 nm and maximized adsorption after about 50 min ($p < 0.05$). Zeta potential measurements confirmed their negative charges (-12 ± 1 mV for T3 and -10 ± 0.7 mV for insulin) (**Figure 2-7D**), suggesting electrostatic interactions with PLL. These results indicate that PLL enhances the cellular bioavailability of insulin and T3, promoting increased browning differentiation of DFATs.

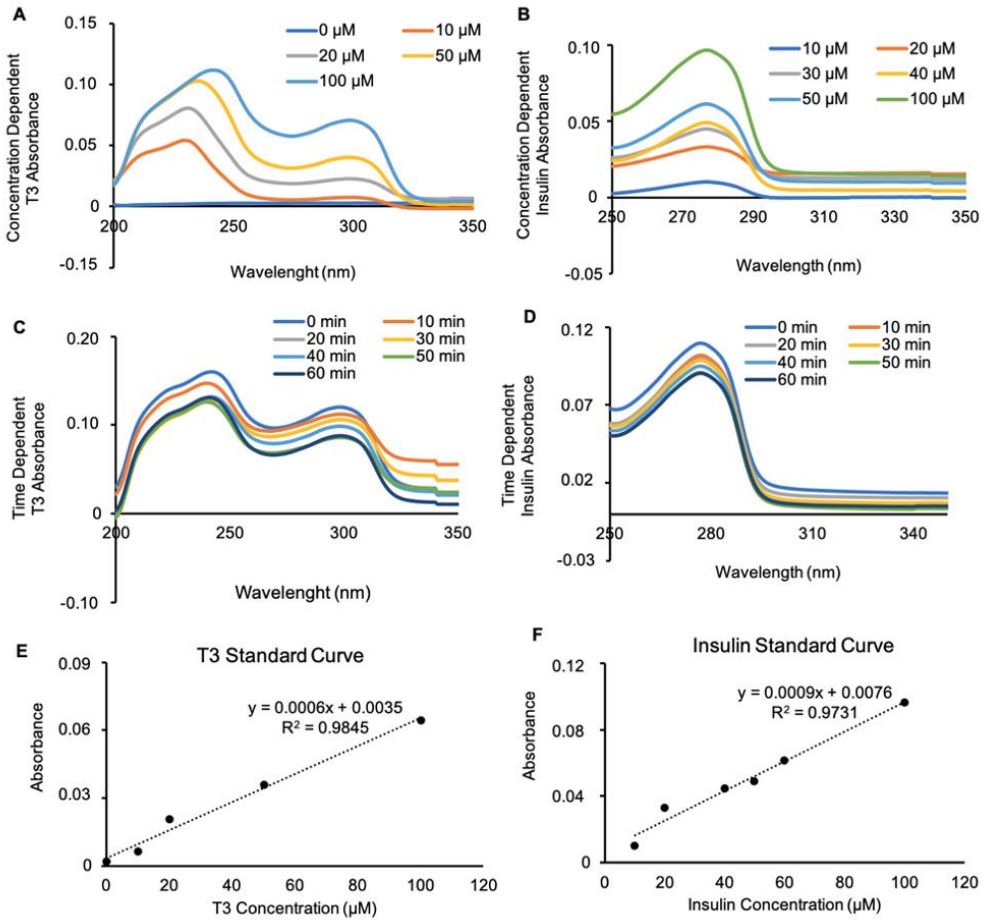


**Figure 2-6.** A. Concentration dependent UV-Vis absorbance spectrum of T3. B. Concentration dependent UV-Vis absorbance spectrum of insulin. C. Time dependent absorbance spectrum of 1 µM T3 solution on PLL coated surface. D. Time dependent insulin absorbance of 10 µM insulin solution on PLL coated surface. E. and F. T3 and insulin standard curves, respectively.

## 2.3.7 PLL integration on DFATs

To confirm the interaction between PLL and DFATs, cells were incubated for 24 h in culture medium with FITC-labeled PLL (green, Figure 2-7C). Since PLL can interact with heparan sulfate proteoglycans (HSPG), HSPG location was also identified by immunostaining. The immunofluorescent images showed an association between the positively charged PLL and the negatively charged HSPG (magenta), suggesting how PLL binds to the cell surface. Figure 6E illustrates the potential mechanism of PLL integration and the increase in brown adipogenic inducing molecules.

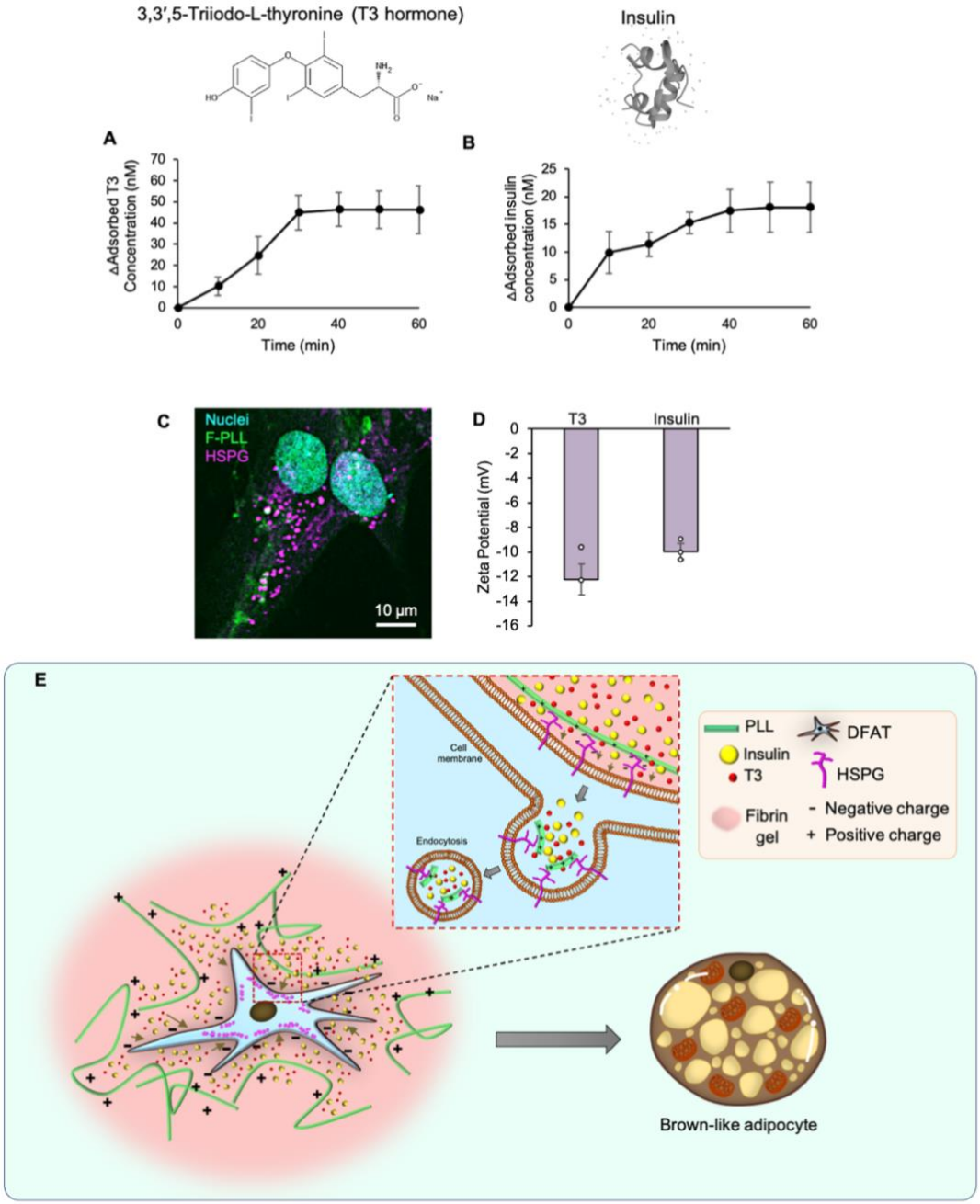


*(Figure caption is on next page.)*

**Figure 2-7.** Conclusion of the study: A) Time-dependent T3 adsorption on PLL-coated surface at 302 nm absorbance (n=3, three independent experiments). B) Time-dependent insulin adsorption on PLL-coated surface at 277 nm absorbance (n=3, three independent experiments). C) Representative HSPG staining image of DFATs incubated in GM with F-PLL (green). HSPG (magenta) and Hoechst counterstaining for nuclei (blue) (Scale bar: 10 μm). D) Zeta potential of T3 and insulin solutions (n=3, three independent experiments). E) Proposed mechanism of DFATs redifferentiation into brown-like adipocytes in PLL-mixed fibrin gel. Positively charged PLL may enhance cellular uptake of T3 and insulin during brown adipogenic induction.

## 2.4 Discussion

In this study, we evaluated the impact of various polymers mixed into a fibrin matrix on browning. Initially, we confirmed that BAM induces brown adipogenic differentiation in DFAT encapsulated in fibrin gel. We analyzed lipid droplet size and metabolic differences such as mitochondrial abundance and oxygen consumption rate. Brown adipocytes had small, multilocular lipid droplets facilitating lipolysis and heat production, with increased mitochondrial activity driven by UCP1. Increased mitochondrial content and UCP1 confirmed successful brown adipogenic differentiation, alongside increased expressions of brown-related mRNAs, including Cidea and PRDM16.

We assessed the impact of various polymers on browning, noting that few studies[15,16,18,24] exist on polymers affecting stem cell adipogenesis signaling, particularly for browning induction. Gonzales-Porras et al. showed ECM-related polymers like collagen type I and laminin decreased brown-like adipocyte differentiation by inhibiting UCP1 expression, which our findings supported.[24] However, co-encapsulation of human MSCs and endothelial cells in collagen type I gel promoted brown adipogenesis.

In our study, we used a medium including T3 and insulin, influencing brown adipogenic differentiation. We found that PLL significantly induced brown adipogenic differentiation compared to other polymers. Immunocytochemical analysis and ELISA assay showed increased UCP1 expression, with mitochondrial analyses confirming significant increases in mitochondrial quantity and oxygen consumption rate due to PLL. Since PLL, a positively charged polymer, likely interacts electrostatically with negatively charged cell surface molecules, facilitating the co-internalization of insulin and T3, crucial for brown adipogenic differentiation. The electrostatic interactions between T3, insulin, and PLL likely enhance

hormone uptake into cells, triggering brown adipogenesis. However, it's unclear if PLL's effects are due to its direct impact on the differentiation process or the mediated hormones.

## 2.5 Conclusion

In conclusion, our study investigated the impact of culture medium and various polymers integrated into the fibrin matrix on brown adipogenic differentiation. We found that incorporating the cationic polymer PLL into the fibrin gel significantly enhanced brown adipogenesis compared to other polymers. The electrostatic interaction between PLL and HSPG on the cell surface likely facilitates the uptake of insulin and T3, promoting brown adipogenic differentiation. Our findings highlight the complex factors influencing brown adipogenesis and identify PLL as a promising candidate for inducing this process. Further research is needed to explore the molecular mechanisms and potential applications of cationic polymers in brown adipogenic differentiation. We hope our study will contribute significantly to future research in this field.

## 2.6 References


1. A. Armani, C. Mammi, V. Marzolla, *J. Cell Biochem*, **2010**, *110*, 564.
2. T. Scully, A. Ettela, D. LeRoith, E.J. Gallagher, *Front Oncol*. **2021**,*10*, 615375.
3. A. O. Silva, M. V. Silva, L. K. N. *J. Pediatr (Rio J)* **2016**, *92*, 174.
4. P. Poirier, T. D. Giles, G. A. Bray, *Circulation*, 2006, *113*, 898.
5. D. Antillon, A. Towfighi, *Women's Health* **2011**, *7*, 454.
6. H. Lee, *Cells* **2022**, *11*, 1472.
7. E. W. Edmonds, K. J. Templeton, *Clin. Orthop. Relat. Res*. **2013**, *47*, 1191.
8. D. A. Fitzgerald, *Paediatr. Respir. Rev*. **2017**, *24*, 4.
9. T. Lobstein, R. Jackson-Leach, J. Powis, *World Obesity Federation*. **2023**.
10. A. Smorlesi, A. Frontini, A. Giordano, *Obesity Reviews* **2012**, *13*, 83.
11. M. Jumabay, *World J. Stem Cells* **2015**, *7*, 1202.
12. M. C. Tanzi, S. Farè, *Expert Rev. Med. Devices* **2009**, *6*, 533.
13. C. S. Murphy, L. Liaw, M. R. Reagan, *BMC Biomed. Eng*. **2019**, *1*, 1.
14. K. Hemmrich, D. von Heimburg, *Expert Rev. Med. Devices* **2006**, *3*, 635.
15. J. H. Hammel, E. Bellas, *Integr. Biol. (Camb)*. **2020**, *12*, 81.
16. K. M. Tharp, A.K. Jha, J. Kraiczy, *Diabetes* **2015**, *64*, 3713.
17. N. C. Negrini, N. Celikkin, P. Tarsini, *Biofabrication* **2020**, *12*, 025001.
18. J. P. Yang, A.E. Anderson, A. McCartney A, *Tissue Eng. Part A* **2017**, *23*, 253.
19. K. Wittmann, S. Dietl, N. Ludwig, *Tissue Eng. Part A*. **2015**, *21*, 1343.
20. F. Louis, S. Kitano, J. F. Mano, M. Matsusaki, *Acta Biomater*. **2019**, *84*, 194.

21. D. Weidlich, J. Honecker, C, Boehm, *Magn. Reson. Med*. **2021**, *86*, 1256.
22. S. N. Shapira, P. Seale, *Obesity* **2019**, *27*, 13.
23. D. Fischer, Y. Li, B. Ahlemeyer, J. Krieglstein, *Biomaterials* **2003**, *24*, 1121.
24. M. A. Gonzales-Porras, K. Stojkova, M. K. Vaicik, *Sci. Rep*. **2021**, *11*, 5442.

# Chapter 3

# Polyelectrolyte Nanofilms on Cell Surface Can Induce Brown Adipogenic Differentiation of DFATs

## 3.1 Introduction

Obesity is a chronic disease characterized by excessive adipose tissue accumulation, leading to numerous health issues, including cardiovascular diseases, type 2 diabetes, and cancer.[1,2] Its increasing global prevalence has made it a significant public health concern, highlighting the importance of adipose tissue research.[3–5] Within this context, recent therapeutic focus has shifted towards BAT, which plays a crucial role in non-shivering thermogenesis by using fat storage to generate heat.[5] Brown adipocytes are rich in mitochondria and contain UCP1, a protein that uncouples ATP production for heat generation.[6] Targeting BAT, therefore, represents a promising strategy for preventing and managing obesity.[7,8]

In addition to brown adipocytes, adipose tissue's plasticity allows mature white fat cells to dedifferentiate into stem cell-like DFAT cells, which can differentiate into various lineages, such as osteogenic, chondrogenic, and adipogenic.[9–11] These DFAT cells have immunomodulatory, regenerative, and therapeutic properties, making them valuable for medical applications.[12–15] Given this potential, reprogramming white adipocytes into BAT through dedifferentiation is crucial for advancements in BAT engineering and regenerative medicine.

To control the differentiation of DFAT into brown adipocytes, the Layer-by-Layer (LbL) coating technique offers a promising solution in tissue engineering. This technique involves constructing ultra-thin coatings by assembling materials or cells one layer at a time, utilizing interactions such as electrostatic, hydrophobic, and biological recognition.[16–18] LbL nanofilms can guide cell behavior, promoting adhesion, migration, proliferation, and activating signaling pathways crucial for cell differentiation.[19–24] Additionally, LbL coatings are fast, versatile, and affordable for tailoring surface properties.

Research on nanofilms has expanded, offering new ways to harness cell behavior for therapeutic purposes. For instance, LbL nanofilms made from collagen type I and hyaluronic

acid have been shown to mimic the extracellular matrix and activate cytoprotective pathways.[23] Similarly, hyaluronic acid and PLL nanofilms can regulate cell adhesion and facilitate the binding of target proteins.[24] Multilayered hyaluronic acid/chitosan nanofilms have also enhanced tenogenesis in degenerative rotator cuff tendons.[19] Although polymer coatings have been shown to promote white adipogenic differentiation,[25,26] no research has yet focused on brown adipogenic differentiation using LbL techniques.

In this study, we aimed to create PE nanofilms on DFAT cells using PLL and Dextran Sulfate (DES). PLL is known for promoting cell adhesion, especially in DFAT cells, as found in our previous research.[27,28] DES has demonstrated good cell biocompatibility and is suitable for LbL polymer assembly.[17] We investigated the brown adipogenic differentiation potential of these PE nanofilm-coated DFAT cells. Previous literature reported that PLL induces white adipogenic differentiation by affecting insulin signaling.[29] Our prior research also found that PLL mixed into fibrin gel could induce brown adipocyte differentiation in DFAT cells by increasing the cellular uptake of T3 and insulin.[27] Building on this, we evaluated whether the PE nanofilm coating further enhances the browning capacity of DFAT cells through immunofluorescent and gene expression analyses.

## 3.2 Experiments

### 3.2.1 Materials

Fibrinogen (F8630), Thrombin (T4648), and Fibronectin (F2006) from bovine and human plasma, Collagen type IV from human placenta (C7521), Poly-L-lysine hydrobromide (P6282) and its FITC conjugated form (P3543), Phosphate Buffered Saline powder (PBS, D5652), Collagenase from Clostridium histolyticum (Type I, C0130), Triton-X 100 (T8787), Bovine Serum Albumin (BSA, 3294), Dexamethasone (D4902), Indomethacin (I7378), 3-Isobutyl-1-methylxanthine (IBMX, I5879), Insulin (I6634), Rosiglitazone (R2408), 3,3′,5-Triiodo-L-thyronine sodium salt (T3, T6397), and Hoechst 33324 (H3570) were purchased from Sigma-Aldrich (St Louis, MO, USA). Trypan Blue (T10282), UCP1 polyclonal antibody (PA1-24894), Anti-rabbit secondary antibody Alexa Fluor® 647, Nile Red (N1142), PicoPureTM RNA Isolation kit (KIT0204), Penicillin, Streptomycin, and HCS LipidTOX™ deep red neutral lipid stain (H34477) were provided from Thermo Fisher Scientific (Waltham, MA, USA) provided. Sodium dextran sulfate 5000 (194-13402), 4%-paraformaldehyde (16310245) and Trypsin were obtained from Fujifilm Wako Pure Chemical Industries (Tokyo,

Japan). Dulbecco's Modified Eagle Medium high glucose (08458-16) and Phosphate Buffer Saline (14249-24) were procured from Nacalai Tesque Inc. (Kyoto, Japan). Fetal Bovine Serum (FBS, 10270106) was obtained from Gibco. RNase-free DNase set (79254) was purchased from Qiagen (Hilden, Germany). iScriptTM cDNA Synthesis Kit was provided from Bio-Rad (California, USA). TaqMan gene expression assays (Applied Biosystems) were purchased from Thermo Fisher Scientific (Waltham, MA, USA). Sodium dextran sulfate rhodamine (DES-Rhodamine-5k) was sourced from HAworks (Bedminster, USA).

### 3.2.2 PE Nanocoating on DFATs

The process of polymer nanocoating on DFATs is demonstrated in **Figure 3-1A**. DFATs were coated using the layer-by-layer adsorption technique with oppositely charged polymers PLL and DES, following established protocols.[30–32] For cells coated with three layers, the protocol involved resuspending $0.5\times10^6$ cells in PBS (pH 7.4) in an Eppendorf tube, followed by centrifugation at 2500 rpm for 1 minute. After removing the supernatant, 500 µL of PLL solution (0.01 or 0.05 µg/mL, prepared in PBS pH 7.4) was added to the cell pellet and mixed. The cells were then rotated at 12 rpm using a microtube rotator (As One, MTR-103/1-4096-01-22) for 1 minute before centrifugation again at 2500 rpm for 1 minute. Following removal of the PLL solution, the cells underwent PBS wash, rotation, and centrifugation. Subsequently, 500 µL of DES solution (0.01 or 0.05 µg/mL) was added similarly, followed by rotation, centrifugation, and PBS wash with centrifugation. Finally, another 500 µL of PLL solution (0.01 or 0.05 µg/mL) was applied before a final PBS wash and centrifugation. Additional layers followed the same PLL, PBS, DES, PBS sequence. Cells intended for single-layer coating received only the initial PLL application. The coated cells were then prepared for further analysis or experimental use.

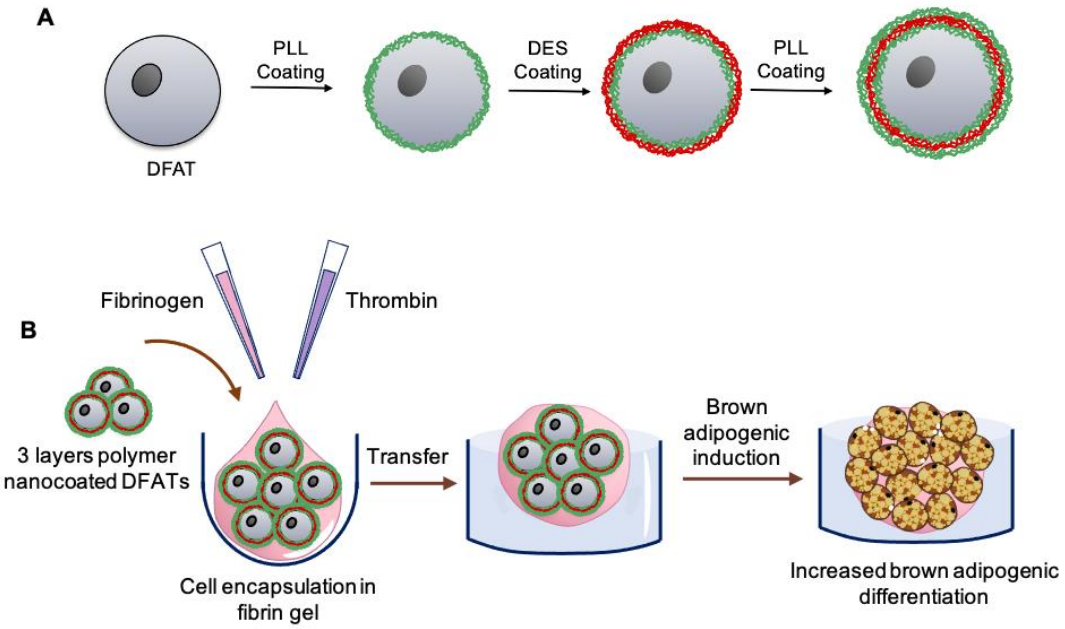


**Figure 3-1.** Schematic representation of the study. A) DFATs underwent coating using PLL and DES via layer-by-layer assembly. B) Polymer-coated DFATs were embedded in fibrin gel in a 96-well round bottom plate to form spherical drops. These drops were then transferred to a 24-well ultra-low attachment plate and incubated in brown adipogenic differentiation medium for 14 days. (PLL: Poly-L-lysine, DES: Dextran Sulfate)

### 3.2.3 Cell viability measurement

Following the application of polymer coatings, cell viability was evaluated using Trypan Blue staining and a cell Countess 3 (Invitrogen, Thermo Fisher Scientific, Waltham, MA, USA).

### 3.2.4 Brown adipogenic differentiation of nanofilm coated DFATs

**Figure 3-1B** illustrates the procedural outline for sample preparation. In the 3D culture, DFATs coated with one or three layers of polymer were combined at a seeding density of $4.0\times10^6$ cells/mL with a fibrinogen solution (final concentration 6 mg/mL, prepared from a 50 mg/mL stock in DMEM with 0% FBS and 1% penicillin-streptomycin, filtered through a 0.2 µm filter). Subsequently, a thrombin solution (final concentration 3 U/mL, from a 10 U/mL stock in DMEM with 10% FBS and 1% penicillin-streptomycin, also filtered through a 0.2 µm filter) was added. The resulting mixture was seeded into a 96-well ultra-low attachment round-bottom plate (IWAKI, EZ-BindShutTM II, 4870-800LP) using wide pipette tips, dispensing 5 µL per well, and incubated at 37 °C for 20 minutes for gelation. After gelation, culture medium

was added to detach the drops, which were then transferred to a 24-well ultra-low attachment plate. Each well received 500 µL of brown adipogenic differentiation medium (BAM) containing dexamethasone (0.5 µM), indomethacin (125 nM), IBMX (250 µM), bovine insulin (850 nM), rosiglitazone (1 µM), triiodothyronine (T3, 120 nM), penicillin-streptomycin (1%), and FBS (10%) in high-glucose DMEM.[33]

For 2D samples, polymer-coated cells were seeded onto cell culture-treated plastic ware at a density of $5.0\times10^4$ cells/cm$^2$. Immunofluorescent analysis was conducted using cells seeded into 96-well plates (IWAKI, 3860-096), while Real Time-quantitative Polymerase Chain Reaction (RT-qPCR) analysis utilized 24-well plates (IWAKI, 3820-024). In both 2D and 3D culture conditions, half of the differentiation medium was replaced every 2 days over the 14-day culture period.

### 3.2.5 Fluorescence imaging

Cells coated with fluorescently labeled PLL and DES were seeded at a density of $0.5\times10^5$ cells per 35 mm glass-bottom culture dish and imaged on day 1 using confocal laser scanning microscopy (CLSM) FV3000 system (Olympus, Tokyo, Japan). Immunostaining of both 2D and 3D samples involved washing the samples three times with PBS after a two-week incubation period in BAM. Following this, the samples were fixed overnight at 4°C in a 4% paraformaldehyde solution in PBS. To enhance permeability, samples were treated with 0.05% Triton X-100 in PBS for 15 minutes and incubated for 1 hour at room temperature in 1% BSA in PBS to minimize nonspecific staining. Subsequently, samples were incubated overnight at 4°C with anti-UCP1 antibody diluted 1:500 in 1% BSA. After incubation, Alexa Fluor® 647-conjugated secondary antibodies were applied at a 1:200 dilution for 2 hours at room temperature. Nile Red staining (50 ng/mL final concentration) was used to visualize intracellular lipid accumulation, and Hoechst dye (10 ng/mL final concentration) was used for nuclear counterstaining. Imaging was performed using the FV3000 CLSM system with a 5 µm step size and consistent laser power for 3D samples.

### 3.2.6 Gene expression analysis

Gene expression levels were assessed using RT-qPCR. Total RNA was extracted using a PicoPure™ RNA Isolation Kit as per the manufacturer's instructions. For 3D samples, six drops were combined per replicate, while for 2D samples, cells from three wells were pooled

to form each replicate. The concentration of RNA was determined with a NanoDrop™ N1000 spectrophotometer. RNA was converted to cDNA using an iScript cDNA Synthesis Kit following the manufacturer's protocol. Subsequently, cDNA amplification was performed using TaqMan Fast Advanced Master Mix and TaqMan Gene Expression Assays targeting UCP1, Cidea, PRDM16, and RPII (used as the housekeeping gene) following manufacturer protocols (Supplementary Table 1). Both cDNA synthesis and RT-qPCR reactions were carried out using a StepOnePlus Real-Time PCR System.

### 3.2.7 PE nanofilm fabrication monitoring via quartz crystal microbalance (QCM)

PE nanofilm fabrication was monitored using a 27 MHz quartz crystal microbalance (QCM) (AFFINIX Q8, ULVAC). Gold-coated QCM sensors (QCM01S, ULVAC) underwent cleaning with piranha solution ($H_2SO_4$: 35% $H_2O_2$ = 3:1) for 10 minutes, repeated three times, followed by three washes with Milli-Q water. Subsequently, PBS solution (100 µL, pH: 7.4) at 37°C was applied until the frequency stabilized. A PLL solution (5 µL, pH: 7.4, in PBS) was then introduced onto the sensors, and frequency changes were monitored. After a 15-minute deposition, the sensors were rinsed thrice with Milli-Q water (pH: 7.4) and stabilized in PBS (100 µL). Then, DES solution (5 µL, pH: 7.4, in PBS) was added to deposit the second layer. This alternating process of polymer solutions facilitated the layer-by-layer (LbL) assembly of nanofilms. The mass adsorbed (Δm) was calculated using the Sauerbrey equation:

$$-\Delta m\ (ng/cm^{-2}) = 0.62 \times \Delta F(Hz) \quad (1)$$

### 3.2.8 Atomic force microscopy (AFM) observation

PE nanofilms were created on silicon wafers and analyzed for surface morphology using AFM under wet conditions at room temperature (Shimadzu, SPM-Nanoa). Two different concentrations of polymer coating, 0.05 µg/mL and 0.01 µg/mL, were examined. The silicon wafers were subjected to a 10-minute plasma treatment before the film fabrication process.

### 3.2.9 Monitoring of T3 and insulin adsorption on PE nanocoated surfaces

A 3-layer PE nanofilm coating process was performed on a 96-well polystyrene surface using PLL and DES at a concentration of 100 µg/mL (in PBS, pH: 7). Subsequently, T3 (1 mM)

and insulin (1 mM) solutions were prepared as per the manufacturer's instructions and applied to the PE nanocoated surfaces and control wells (coated with Milli-Q water) at 100 µL per well. After a 1-hour incubation at 37°C, absorbance measurements at 302 nm for T3 and 277 nm for insulin were taken using a plate reader. The amount of adsorbed product on the surface was quantified by comparing absorbance values against standard curves for T3 and insulin.

***Statistical Analysis*:** ANOVA analyses were performed using ezANOVA software to detect significant differences among pairs of datasets. Error bars were used to represent standard deviation, with statistical significance defined as *p*-values below 0.05.

## 3.3 Results

### 3.3.1 Cell viability assessment after PE nanocoating on DFATs

Due to the high cytotoxicity of polycations,[34] particularly PLL, its concentration was optimized to determine the ideal cell viability. DFAT cells were coated with PLL solutions ranging from 0.01 to 20 µg/mL, and cell viability post-coating was assessed with Trypan Blue staining. Results indicated that only concentrations of 0.01 and 0.05 µg/mL maintained cell viability rates of 70% or higher (**Figure 3-2**). Consequently, subsequent cell culture experiments were conducted using these concentrations. The influence of varying the number of coated layers on cell viability was then examined. It was observed that for both 0.01 and 0.05 µg/mL concentrations, cell viability significantly dropped to below 20% after the third layer in cells coated with 1, 3, and 5 layers of PE (**Figure 3-3A**). Therefore, experiments proceeded with 1 and 3 layers of coating.

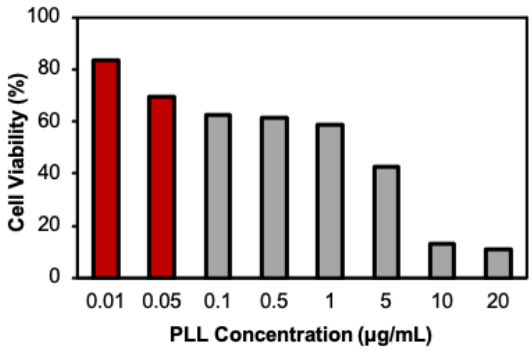


**Figure 3-2.** Cell viability was assessed using Trypan Blue staining and cell counting after applying a single layer of PLL nanocoating. The experiments were conducted with a sample size of n=1, using one independent sample from a single donor.

### 3.3.2 Film thickness measurement

The thickness of PE nanofilms was initially examined using QCM. **Figure 3-2B** illustrates that film thickness increased with higher polymer solution concentrations. Specifically, at 0.01 and 0.05 µg/mL, three layers resulted in film thicknesses of 0.56 (± 0.13)

nm and 0.94 (± 0.29) nm, respectively, while a concentration of 1 µg/mL produced a thickness of 1.9 (± 0.45) nm. By the seventh layer, a concentration of 0.05 µg/mL yielded a film thickness of 3.7 (± 0.7) nm. AFM data in **Figures 3-2C** and **D** revealed a similar film thickness profile of 3.03 nm for seven layers at 0.05 µg/mL. Increased polymer concentration intensified electrostatic interactions among polymer chains, resulting in thicker films.

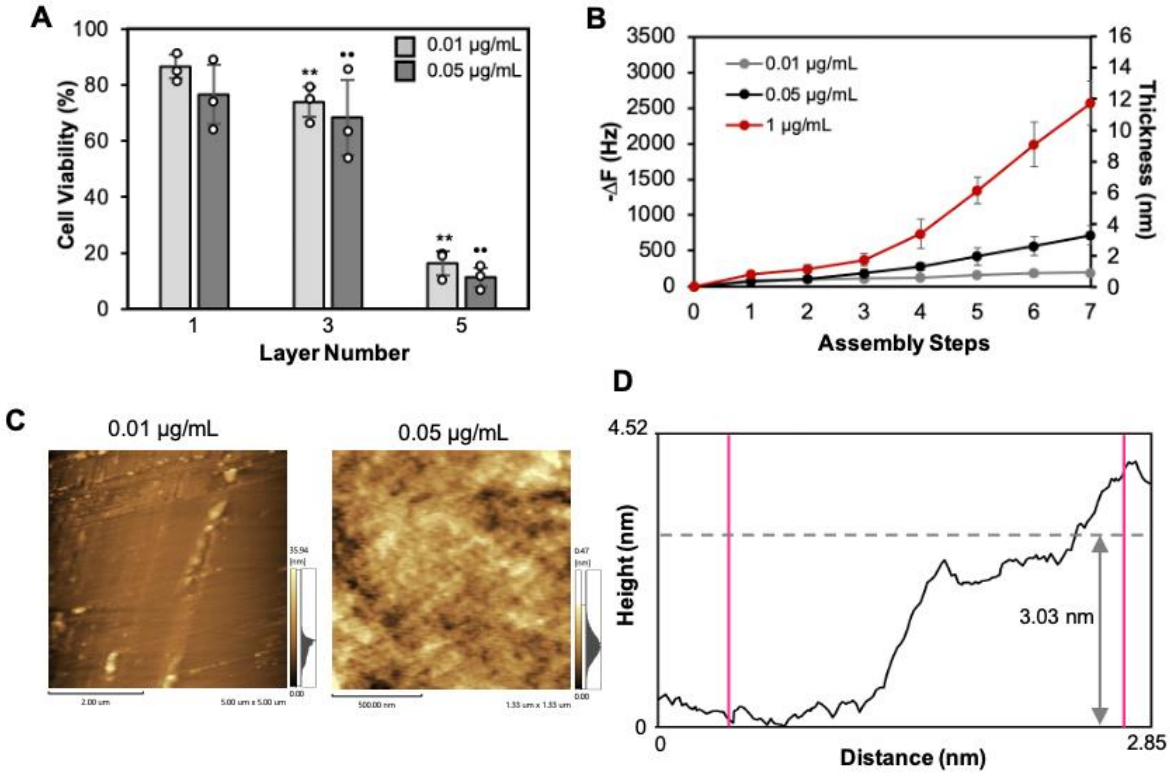


**Figure 3-3** Polymer nanocoating assessment. A) Cell viability was assessed using Trypan Blue staining and cell counting after applying the polymer nanocoating. Results are presented with standard deviation (± s.d.) from experiments conducted with n=3, using three independent samples from a single donor. Statistical differences, determined by ANOVA, are indicated as ** ($p < 0.01$) when comparing to one layer 0.01 µg/mL, and •• ($p < 0.01$) when comparing to one layer 0.05 µg/mL. Each white dot represents data points from individual replicates. B) Quartz crystal microbalance (QCM) analysis shows frequency shift and thickness of the PLL-DES nanofilm assembly. C) AFM images depict the 7-layer nanocoating assembly. D) Thickness profile of the 7-layered 0.05 µg/mL PLL-DES film on a silicon wafer substrate.

### 3.3.3 Fluorescence imaging of PE nanocoated DFATs

Fluorescently labeled polymer coating confirmed the nanofilm presence on cells. **Figure 3-4A** shows DFATs coated with fluorescently labeled PLL and DES imaged on day 1 after PE nanocoating using CLSM. The line scanning results shown in **Figure 3-4B** confirmed the coating by identifying regions with and without fluorescent signals. Green lines depict FITC-labeled PLL fluorescence, while red lines depict Rhodamine-labeled DES fluorescence. Increasing the polymer concentration from 0.01 to 0.05 µg/mL led to approximately a 20% increase in fluorescence intensity in the line scanning results.

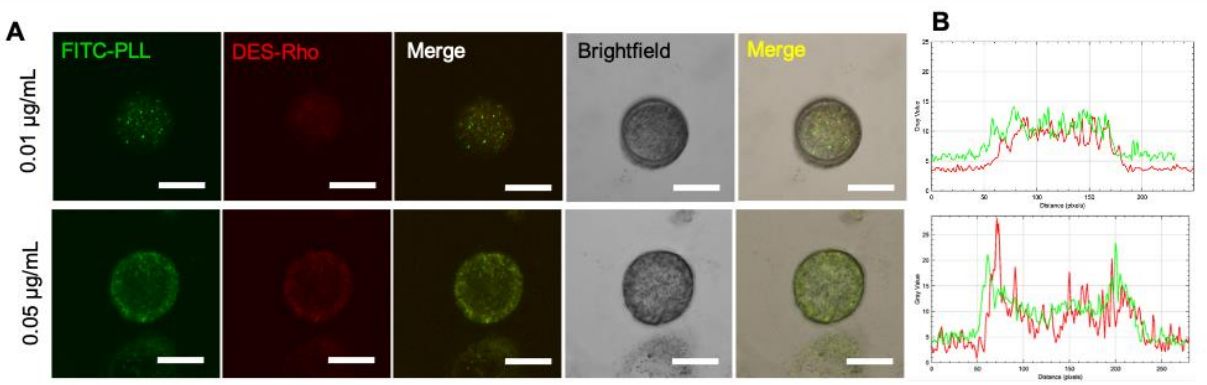


**Figure 3-4** A) Immunofluorescence images show a representative DFAT cell coated with three layers of fluorescent-labeled PLL-DES (Scale bar: 20 µm). B) Line scanning results for DFAT cells coated with three layers of fluorescent-labeled PLL-DES.

### 3.3.4 2D Brown adipogenic redifferentiation

After confirming PE nanocoating on the cells, their brown adipogenic differentiation was initially assessed on polystyrene 2D cell culture plates using immunofluorescence and gene expression analyses. Nanocoated cells were seeded and cultured in a brown adipogenic differentiation medium for immunofluorescence analysis of UCP1 and lipid droplets, as depicted in **Figure 3-5A**. Quantification of UCP1 and lipid droplets was performed by normalizing their fluorescence intensities to Hoechst-stained cell nuclei (**Figure 3-5B**). The UCP1 content in cells coated with 3 layers of 0.01 and 0.05 µg/mL PLL did not significantly differ from the control group (uncoated cells), as shown by the gray bars in **Figure 3-5B**. Similarly, among the experimental groups, only cells coated with a single layer of 0.05 µg/mL PLL exhibited increased lipid intensity. However, since lipid content alone is insufficient to

determine browning status, gene expression related to BAT such as UCP1, Cidea, and PRDM16 was also evaluated. According to the gene expression results in **Figure 3-6**, there was no significant increase in the expression of these genes in PE-coated cells compared to uncoated groups. Therefore, it is evident that the 2D culture conditions did not significantly promote brown adipogenic differentiation of PE nanocoated cells.

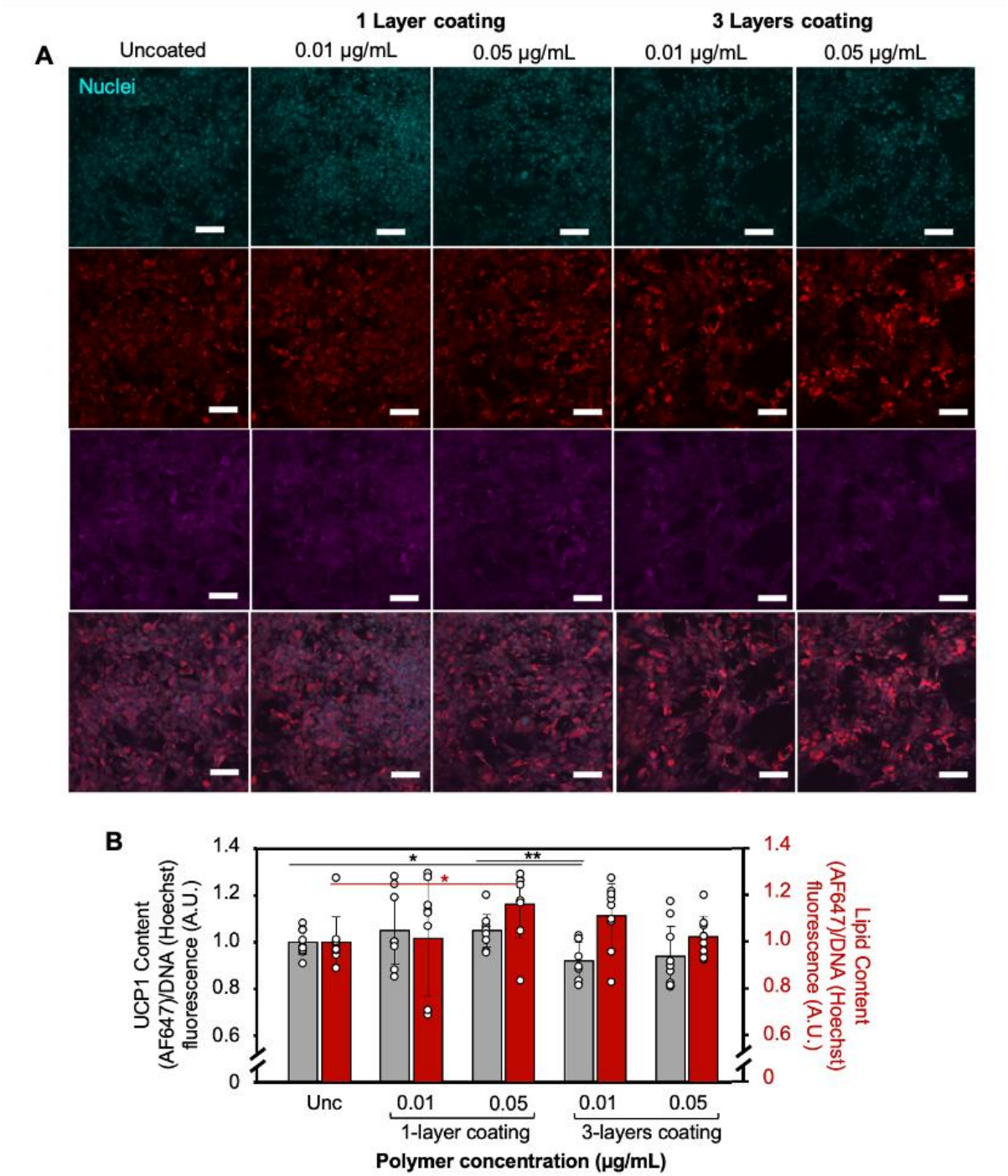


*(Figure caption is on next page.)*

**Figure 3-5.** A) Immunocytochemical staining images of UCP1 (magenta), Nile Red-stained lipid droplets (red), and Hoechst-stained nuclei (blue) are presented for PE nanocoated DFATs seeded on a 96-well plate at day 14. The Merge image combines UCP1, lipid droplets, and nuclei of cells (Scale bar: 200 µm). B) UCP1 (grey bars) and Nile Red fluorescence intensity of lipid droplets (red bars), normalized to Hoechst-stained DNA fluorescence, are shown as mean ± standard deviation (n=3, from three independent samples of one donor). Statistical significance was determined using ANOVA tests, with * indicating $p < 0.05$. (Unc: Uncoated)

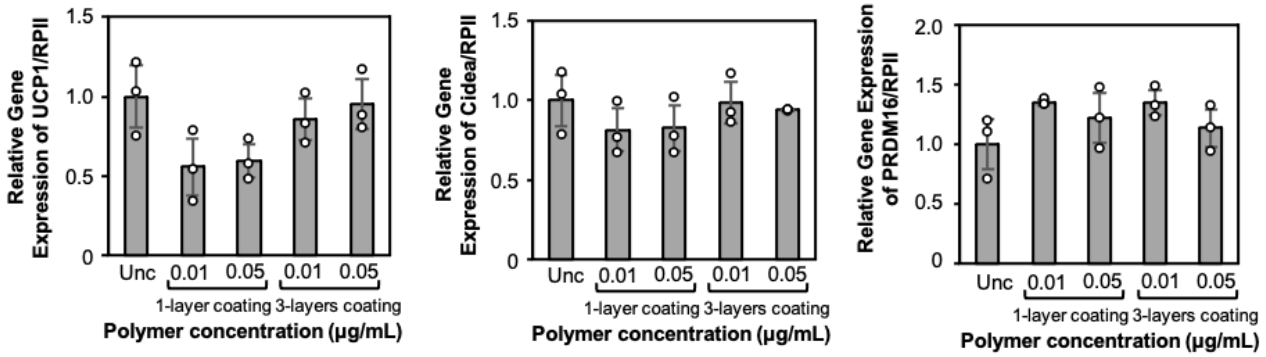


**Figure 3-6.** The relative gene expressions of brown adipogenic markers UCP1, Cidea, and PRDM16 are displayed as mean ± standard deviation (n=3, from three independent samples of one donor) for PE nanocoated DFATs seeded on a 96-well plate at day 14. Statistical significance was assessed using ANOVA tests, denoted by * indicating $p < 0.05$. Each white dot represents data points from individual parallels. (Unc: Uncoated).

### 3.3.5 3D Brown adipogenic redifferentiation

The brown adipogenic differentiation of PE nanocoated cells in 3D was evaluated by encapsulating them in fibrin gel and culturing them in differentiation medium for 2 weeks, followed by immunofluorescence staining (**Figure 3-7A**). Analysis of lipid content in the stained droplets (**Figure 3-7B**, red bars) revealed no significant differences among the groups. However, quantitative assessment of UCP1 content showed an approximately 1.5-fold increase in cells coated with 3 layers of 0.05 µg/mL PE nanocoating, though this was not statistically significant. To further analyze browning status, gene expressions of UCP1, Cidea, and PRDM16 were evaluated. Cells coated with 3 layers of both 0.01 and 0.05 µg/mL PE showed approximately a 1.5-fold increase in UCP1 gene expression, with statistical significance observed in the 0.05 µg/mL PE coated groups (**Figure 3-8**). Cidea gene expression showed a slight increase in 0.05 µg/mL 3-layer coated cells compared to uncoated cells. PRDM16 also exhibited a similar increase in both the 0.01 and 0.05 µg/mL 3-layer coated groups, although it

was not statistically significant. These findings suggest that PE nanocoating potentially enhances the brown adipogenic differentiation of DFAT cells.

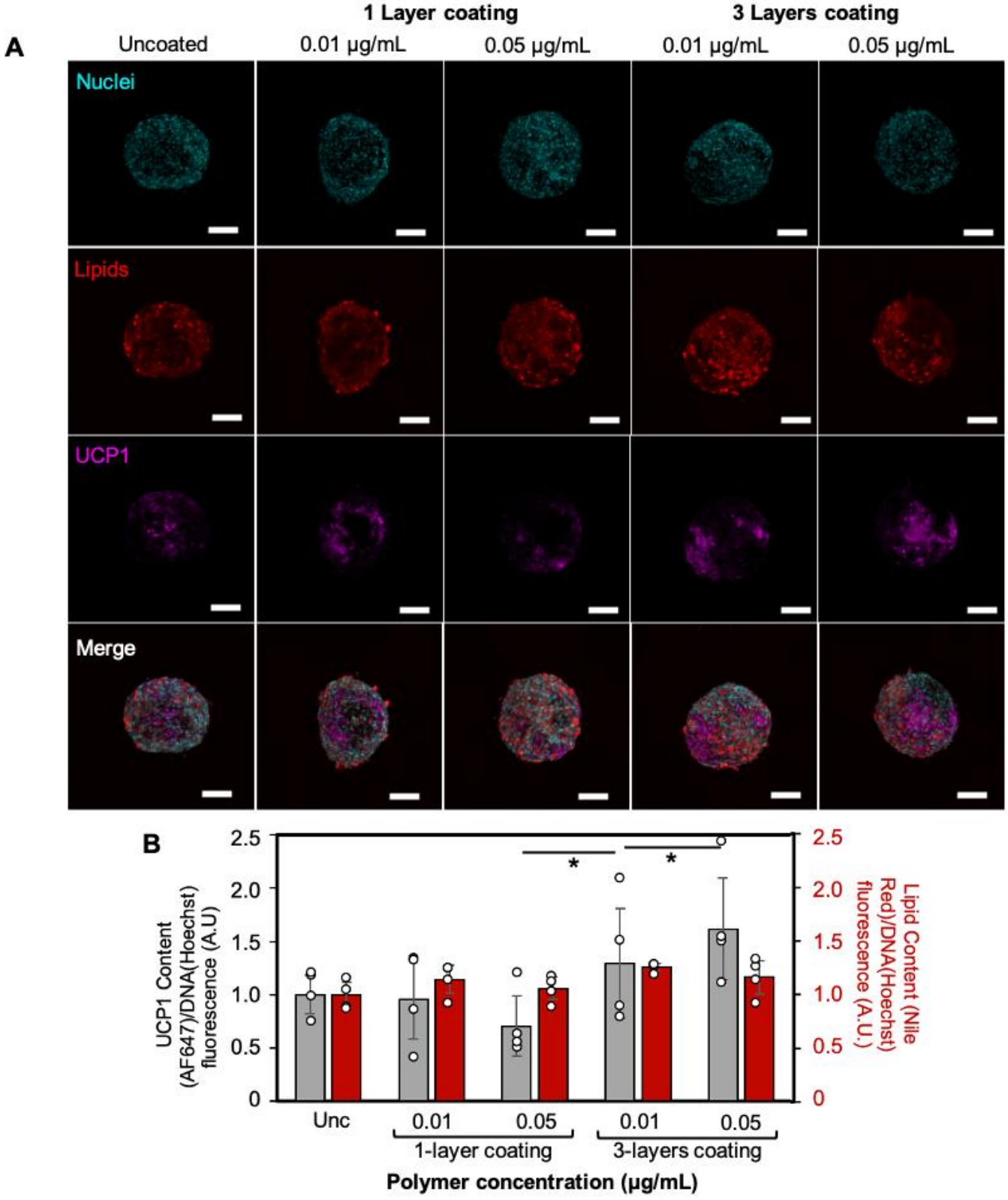


*(Figure caption is on next page.)*

**Figure 3-7.** A) Representative immunocytochemical images showing UCP1 (magenta), lipid droplets stained with Nile Red (red), and nuclei counterstained with Hoechst (blue) are presented for PLL-DES nanocoated DFATs encapsulated in fibrin gel on day 14. The Merge image combines UCP1, lipid droplets, and nuclei of cells (Scale bar: 200 µm). B) Measurements of UCP1 (grey bars) and Nile Red fluorescence of lipid droplets (red bars), normalized to DNA fluorescence (Hoechst), are reported as mean ± standard deviation (n=3, from three independent samples of one donor). Statistical significance was determined using ANOVA tests and is indicated by * = $p < 0.05$.

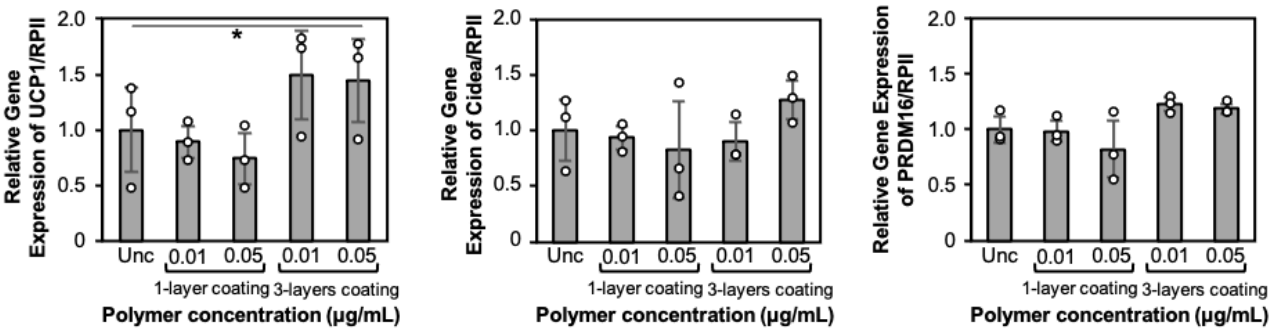


**Figure 3-8.** At day 14, the gene expressions of brown adipogenic markers UCP1, Cidea, and PRDM16 for 3D samples are shown as mean ± standard deviation (n=3, from three independent samples of one donor). Statistical significance was assessed using ANOVA tests, with indic

### 3.3.6 T3 and insulin adsorption on PLL coated surfaces

As a cationic polymer, PLL interacts with components of the differentiation medium that carry a negative charge, potentially facilitating their adsorption and thereby promoting brown adipogenic differentiation. To test this, T3 and insulin solutions were added to 96-well plates coated with 1 and 3 layers of PE. UV absorbance was measured at 1-hour intervals using a plate reader. Based on standard curves for T3 and insulin (**Figure 3-9**), we calculated their adsorption on PE-coated surfaces. Results showed that on a single layer of PLL, T3 and insulin adsorbed up to 62 (± 18) µM and 70 (± 12) µM, respectively. On surfaces coated with three layers of PE, adsorption increased to 80 (± 12) µM and 104 (± 28) µM, respectively (**Figure 3-10A**). These findings indicate that increasing the number of layers enhances the electrostatic charge density, leading to greater adsorption of negatively charged components. Thus, the mechanism proposed in **Figure 3-10B** suggests that direct PE nanofilm coating on cell surfaces may enhance cellular uptake of T3 and insulin, thereby promoting browning.

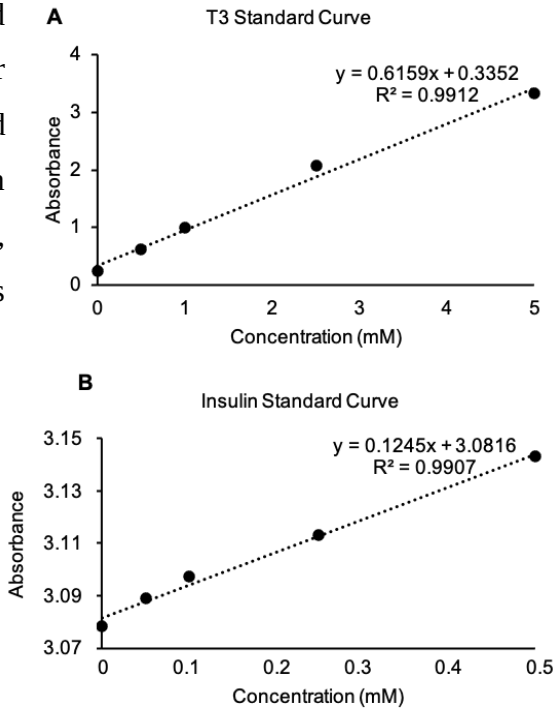


**Figure 3-9.** A) T3, B) Insulin standard curves by measured with plate reader at 302 nm and 277 nm, respectively.

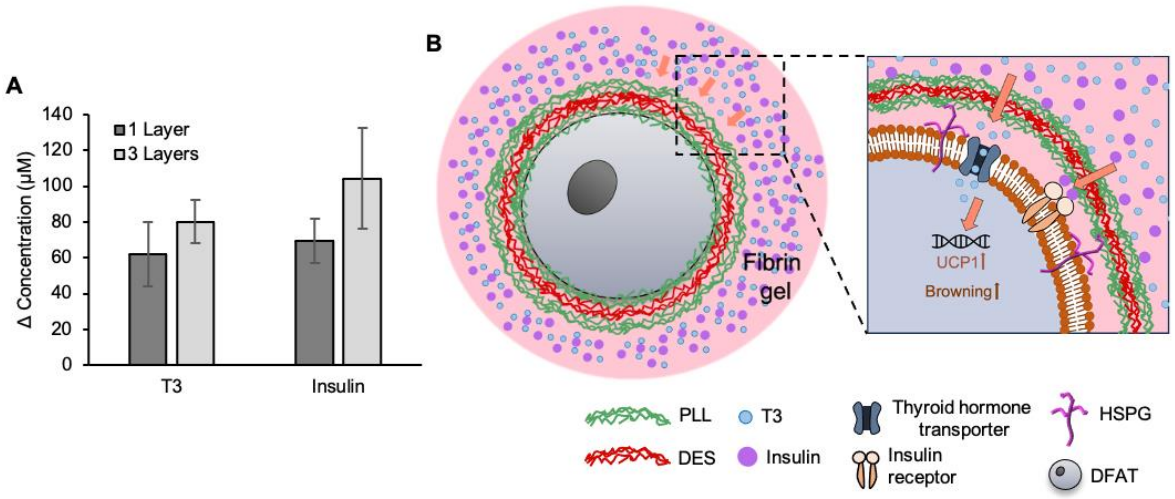


**Figure 3-10.** A) T3 and insulin adsorption on a PLL-DES coated surface was monitored at 302 nm and 277 nm, respectively, after a 1-hour incubation at 37°C (n=3, independent experiments). B) The proposed mechanism suggests that polyelectrolyte nanocoating enhances brown adipogenic differentiation in DFATs by increasing cellular uptake of T3, thereby upregulating brown adipose tissue-related gene expressions.

## 3.4 Discussion

In this study, the impact of PE nanocoating, comprising PLL and DES, on the brown adipogenic differentiation of DFAT cells in both 2D and 3D cultures was inventigated. Previously, we demonstrated that PLL could enhance brown adipogenic differentiation by facilitating the uptake of insulin and T3, essential components of the differentiation medium. T3 is known to potentiate the effects of norepinephrine in vivo, stimulating brown adipocyte thermogenesis via a cAMP-mediated pathway. Similarly, insulin influences adipogenic differentiation by modulating pathways like AMPK when combined with T3 *in vitro*. Therefore, their synergistic use is critical for promoting brown adipogenesis.

To determine the optimal PLL concentration for cell viability, we assessed different concentrations ranging from 0.01 to 0.05 µg/mL, identifying that 0.01 and 0.05 µg/mL PLL maintained cell viability above 70%. Lower concentrations minimize potential cytotoxic effects associated with polycations, which can disrupt cell membranes or induce oxidative stress. Additionally, we found that maintaining viability above 70% was feasible up to 3 layers of nanocoating, beyond which viability significantly dropped to around 20%, likely due to shear stress during serial centrifugation.

The film thickness and layer assembly were confirmed using QCM and AFM. AFM proved challenging for films deposited at 0.01 µg/mL due to their ultra-thin nature, falling below the instrument's sensitivity range. Thus, film thickness measurements were restricted to concentrations starting from 0.05 µg/mL from the 7th layer onward.

After confirming successful nanofilm deposition on cells, we evaluated their brown adipogenic potential in both 2D and 3D cultures. Notably, 3D cultures demonstrated superior induction of browning compared to 2D environments. This advancement is attributed to the ability of 3D settings to better simulate in vivo conditions, promoting enhanced cellular interactions and metabolic activities conducive to adipogenic differentiation. Moreover, 3D drops embedded in fibrin gel are widely used in adipose tissue engineering for mimicking cell mechanotransduction. While fibrin gel supports a 3D structure, it does not directly contribute to adipogenic differentiation. Therefore, this study focused on how PE coating enhances brown adipogenesis by facilitating the uptake of negatively charged differentiation medium components such as insulin and T3.

Finally, we confirmed brown adipogenic induction in PE-coated cells through increased UCP1 expression, indicating successful differentiation. While similar trends were observed for Cidea and PRDM16, these early gene markers may have shown non-significant changes due to their timing compared to UCP1, which is expressed later in the differentiation process.

## 3.5 Conclusion

This study showed that PE nanocoating, using PLL and DES, significantly promotes the brown adipogenic differentiation of DFAT cells. It is hypothesized that PLL and DES facilitate the uptake of insulin and T3 hormones, crucial for this differentiation process. In 3D cultures, cells encapsulated in fibrin gel exhibited a more robust increase in brown adipogenic markers compared to 2D cultures, highlighting the superior ability of 3D environments to mimic *in vivo* conditions and support differentiation.

To date, there have been no reports on the differentiation of stem cells coated with PE nanofilms into brown adipocytes. While significant strides have been made in developing LbL assembly scaffolds for tissue engineering, the specific effects of mechanical, physical, and biochemical properties of PE nanofilm layers on cellular functions remain unclear. This

research provides valuable insights into the potential of PE nanofilms to enhance DFAT cell differentiation into brown adipocytes, opening new avenues for tissue engineering applications.

## 3.6 References


1. E. Nigro, O. Scudiero, M. L. Monaco, *Biomed. Res. Int*. **2014**, *2014*, 658913.
2. D. Mohajan, H. K. Mohajan, *J. Innovations Med. Res*. **2023**, *2*, 12.
3. B. Reed, S. Abunnaja, *Handbook of Metabolic and Bariatric Surgery* **2022**, 20.
4. H. Sacks, M. E. Symonds, *Diabetes* **2013**, *62*, 1783.
5. F. W. Kiefer, *Best Pract. Res. Clin. Endocrinol. Metab*. **2016**, *30*, 479.
6. E. T. Chouchani, L. Kazak, B. M. Spiegelman, *Cell Metab*. **2019**, *29*, 27.
7. S. Y. Min, J. Kady, M. Nam, *Nat. Med*. **2016**, *22*, 312.
8. A. J. Whittle, M. López, A. Vidal-Puig, *Trends Mol. Med*. **2011**, *17*, 405.
9. Z. Liang, Y. He, H. Tang, *Stem Cell Res. Ther*. **2023**, *14*, 207.
10. A. S. Karanfil, F. Louis, Y. Sowa, M. Matsusaki, *Biomater. Sci*. **2023**, *11*, 7623.
11. T. Matsumoto, K. Kano, D. Kondo, *J. Cell Physiol*. **2008**, *215*, 210.
12. T. Yanagi, H. Kajiya, S. Fujisaki, *Regen. Ther*. **2021**, *18*. 472.
13. T. Kazama, M. Fujie, T. Endo, *Biochem. Biophys. Res. Commun*. **2008**, *377*, 780.
14. N. Kakudo. T. Kishimoto, Y. Matsuyama, T. Momota, *Cytotechnology* **2018**, *70*, 948.
15. M. Jumabay, *World J. Stem Cells* **2015**, *7*, 1202.
16. M. Matsusaki, H. Ajiro, T. Kida, T. Serizawa, M. Akashi, *Advanced Materials* **2012**, *24*, 454.
17. K. Kadowaki, M. Matsusaki, M. Akashi, *Chem. Lett*. **2012**, *41*, 523.
18. J. Zeng, M. Matsusaki, *Polym. Chem*. **2019**, *10*, 2960.
19. F. Han, P. Zhang, X. Wen, C. Lin, *Biomater. Sci*. **2019**, *7*, 4388.
20. B. K. Ekambaram, M.S. Niepel, B. Fuhrmann, *ACS Biomater. Sci. Eng*. **2018**, *4*, 1820.
21. F. Gaudière F, I. Masson, S. Morin-Grognet, *Soft Matter*. **2012**, *8*, 8327.
22. M. S. Niepel, B. K. Ekambaram, C. E. H. Schmelzer, *Nanoscale* **2019**, *11*, 2878.
23. D. Choi, J. Heo, J. Hong, *Langmuir* **2021**, *37*, 4587.
24. J. Hwang, D. Choi, M. Choi, *ACS Appl. Mater. Interfaces* **2018**, *10*, 17685.
25. H. Kindi, C. Willems, M. Zhao, *ACS Biomater. Sci. Eng*. **2022**, *8*, 4327.
26. A. Shridhar, A.Y. L. Lam, Y. Sun, *Biotechnol J*. **2020**, *15*, e1900118.
27. A. S. Karanfil, F. Louis, Y. Sowa, M. Matsusaki, *Mater. Today Bio*. Published online 2024.
28. S. Bozzaro, *Methods Mol, Biol*. **2006**, *346*, 446.
29. K. W. Lee, Y. J. An, J. Lee, *Amino Acids* **2021**, *53*, 587.
30. K. Kadowaki, M. Matsusaki, M. Akashi, *Langmuir* **2010**, *26*, 5670.
31. M. Matsusaki, K. Kadowaki, Y. Nakahara, *Angewandte Chemie - International Ed*. 2007, 46, 4689.
32. J. Zeng, M. Matsusaki, *Anal. Sci*. **2021**, *37*, 491.
33. J. P. Yang, A.E. Anderson, A. McCartney A, *Tissue Eng. Part A* **2017**, *23*, 253.
34. D. Fischer, Y. Li, B. Ahlemeyer, J. Krieglstein, T. Kissel, *Biomaterials* **2003**, *24*, 1121.

# Concluding Remarks

In this thesis, the author describes a two-step strategy: first, the dedifferentiation of white adipocytes, followed by their polymer-assisted redifferentiation into brown adipocytes.

Adipose tissue is highly plastic, making it a valuable resource for tissue engineering and regenerative medicine applications. Due to this high plasticity, under appropriate conditions, white adipocytes can lose their lipid content and transform into fibroblastic stem cells, referred to as DFAT cells. In this study, the primary goal was to enhance the efficiency of adipocyte dedifferentiation by modifying the commonly used ceiling culture method through the polymer coating of the inner surface of cell culture flasks. Specifically, the ECM and BM polymers (Col I, Fib, Col IV, and Lam) and cationic polymers (PLL and PDDA) increased dedifferentiation efficiency by promoting the adhesion of adipocytes and serum proteins with adhesive properties to the polymer-coated surface. Conversely, coating the inner surfaces of the flasks with anionic polymers (Gel and GG) reduced cell adhesion due to electrostatic repulsion, thus decreasing the dedifferentiation rate. Therefore, the first stage of this thesis demonstrates, for the first time in the literature, that the dedifferentiation of white adipocytes can be controlled through polymer coating.

In the second step, the focus was on the *in vitro* production of BAT, a tissue type that offers therapeutic potential for metabolic disorders such as obesity and diabetes. BAT's primary function is thermoregulation, during which it consumes calories, making it a natural therapeutic target for treating disorders arising from excess energy accumulation, like obesity. In this part of the thesis, the aim was to redifferentiate DFAT cells obtained from the first phase into brown adipocytes. To achieve this, cells were encapsulated in fibrin gel, with the polymers used in the first phase individually mixed into the gel to prepare the samples. The encapsulated cells were then cultured in a brown adipogenic differentiation medium to generate BAT samples. When evaluating the effects of the mixed polymers on browning, findings obtained through RT-qPCR, immunofluorescent imaging, ELISA assay, and mitochondrial assessment revealed that PLL exhibited a significant browning-inducing effect. This suggests that the cationic polymer PLL may enhance browning by increasing the uptake of negatively charged components in the differentiation medium into the cells.

.

In the third part of the thesis, due to PLL's ability to induce brown adipogenic differentiation, DFAT cells were coated with a nanofilm composed of PLL and DES. The effects of these film coatings on brown adipogenic differentiation were then evaluated. Results indicated that DFATs coated with three PE layers and encapsulated in fibrin gel exhibited homogeneous differentiation and a significant increase in the brown adipogenic marker UCP1 gene expression and content, both of which increased by 1.5 times. Additionally, T3 and insulin, which are crucial for brown adipogenesis, were adsorbed onto the PE films surfaces. This enhanced browning by increasing the cellular uptake of T3 and insulin. This PLL-based PE nanofilm coating on DFAT surfaces represents a novel and significant technology for promoting homogeneous brown adipogenesis in regenerative medicine and healthcare.

# List of Publications

**Chapter 1**

1. ECM Proteins and Cationic Polymers Coating Promote Dedifferentiation of Patient Derived Mature Adipocytes to Stem Cells.
**Aslı Sena Karanfil,** Fiona Louis, Yoshihiro Sowa, Michiya Matsusaki
*Biomater. Sci.* **2023**, 11, 7623-7638.

**Chapter 2**

2. Cationic Polymer Effect on Brown Adipogenic Induction of Dedifferentiated Fat Cells
**Aslı Sena Karanfil,** Fiona Louis, Yoshihiro Sowa, Michiya Matsusaki
*Materials Today Bio.* **2024**, *under revision*.

**Chapter 3**

3. Polyelectrolyte Nanofilms on Cell Surface Can Induce Brown Adipogenic Differentiation of DFATs
**Aslı Sena Karanfil,** Fiona Louis, Yoshihiro Sowa, Michiya Matsusaki
*Materials Today Bio.* **2024**, *submitted*.

**Supplementary publication**

1. Biofabrication of Vascularized Adipose Tissues and Their Biomedical Applications
**Aslı Sena Karanfil,** Fiona Louis, Michiya Matsusaki
*Mater. Horiz.* **2023**, 10, 1539-1558. (Review paper)

# Acknowledgments

This study was carried out from 2021 to 2024 at Department of Applied Chemistry, Graduate School of Engineering, Osaka University. Throughout these three years, I have received a lot of assistance and support both academically and personally. As I conclude this thesis, I wish to extend my heartfelt appreciation to all individuals who have contributed to my journey.

I am deeply grateful to my supervisor, Prof. Michiya Matsusaki, first and foremost for his kindness, patience, effective scientific guidance, unwavering support, and invaluable advice throughout my research journey. I am also profoundly impressed by his exceptional expertise, exemplary time management skills, and broad and unique perspective. By accepting me as a PhD student in his laboratory, he has provided me with the most significant opportunity of my academic career.

I am deeply grateful to the members of my thesis committee, Prof. Kazuya Kikuchi and Prof. Mamoru Fujitsuka, for their insightful comments and generous allocation of time. I would also like to extend my sincere thanks to Assistant Prof. Fiona Louis for her kind and insightful comments, as well as her valuable suggestions during the experiment, data discussion, and article writing process.

In addition to my supervisor, I am deeply grateful to Assistant Prof. Masahiko Nakamoto for his insightful comments on my research. I also extend my thanks to Dr. Naoko Sasaki, and Dr. Quentin Muller for their valuable comments and suggestions on my experiments

I would like to express my heartfelt gratitude to Ms. Eri Enomoto and Ms. Chika Sugiki for their invaluable assistance with laboratory affairs and their support in daily life.

I would also like to thank the previous and current members in the laboratory: Assistant Prof. Kenta Homma, Dr. Zeng Jinfeng, Dr. Yucheng Shang, Ms. Mizuho Suzuki, Ms. Asuka Kato, Dr. Marie Piantino, Ms. Yukiko Sorayama, Ms. Yuka Yoshinouchi, Mr. Koichi Hattori, Mr. Daisuke Tomioka, Ms. Zhang Zhuying, Mr. Yuki Koba, Mr. Kazuki Moroishi, Mr. Kazuki Yoshida, Mr. Tamaki Kumauchi, Ms. Sukulya Bunuasunthon, Mr. Rentaro Sakamoto, Mr. Ryoto Itani, Mr. Kanta Iwamoto, and others. I am grateful for their companionship and generous assistance, both in research and daily life.

I would like to thank the Ministry of Education, Culture, Sports, Science and Technology of Japan for their financial support through the Monbukagakusho (MEXT) Scholarship program.

Finally, I would like to express my deepest gratitude to my parents, Memduha Karanfil and Ahmet Tarık Karanfil, who have been my greatest supporters throughout the completion of my thesis, standing by me with their emotional encouragement and helping me overcome every challenge.

July 2024

Aslı Sena Karanfil